714483

NAVAL SHIP RESEARCH AND DEVELOPMENT CENTER
Washington, D.C. 20034

INFLUENCE OF ADDED MASS ON THE NATURAL VIBRATIONS AND IMPULSE RESPONSE OF LONG, THIN CYLINDRICAL SHELLS

by

E. N. Palmer

DEPARTMENT OF STRUCTURAL MECHANICS
RESEARCH AND DEVELOPMENT REPORT

Report 3395

The Naval Ship Research and Development Center is a U.S. Navy center for laboratory effort directed at the improvement of ships and air vehicles. It was formed in March 1967 by merging the David Taylor Model Basin at Carderock, Maryland and the Marine Engineering Laboratory (now Naval Ship R & D Laboratory) at Annapolis, Maryland. The Mine Defense Laboratory (now Naval Ship R & D Laboratory) Panama City, Florida became part of the Center in November 1967.

Naval Ship Research and Development Center
Washington, D.C. 20034

MAJOR NSRDC ORGANIZATIONAL COMPONENTS

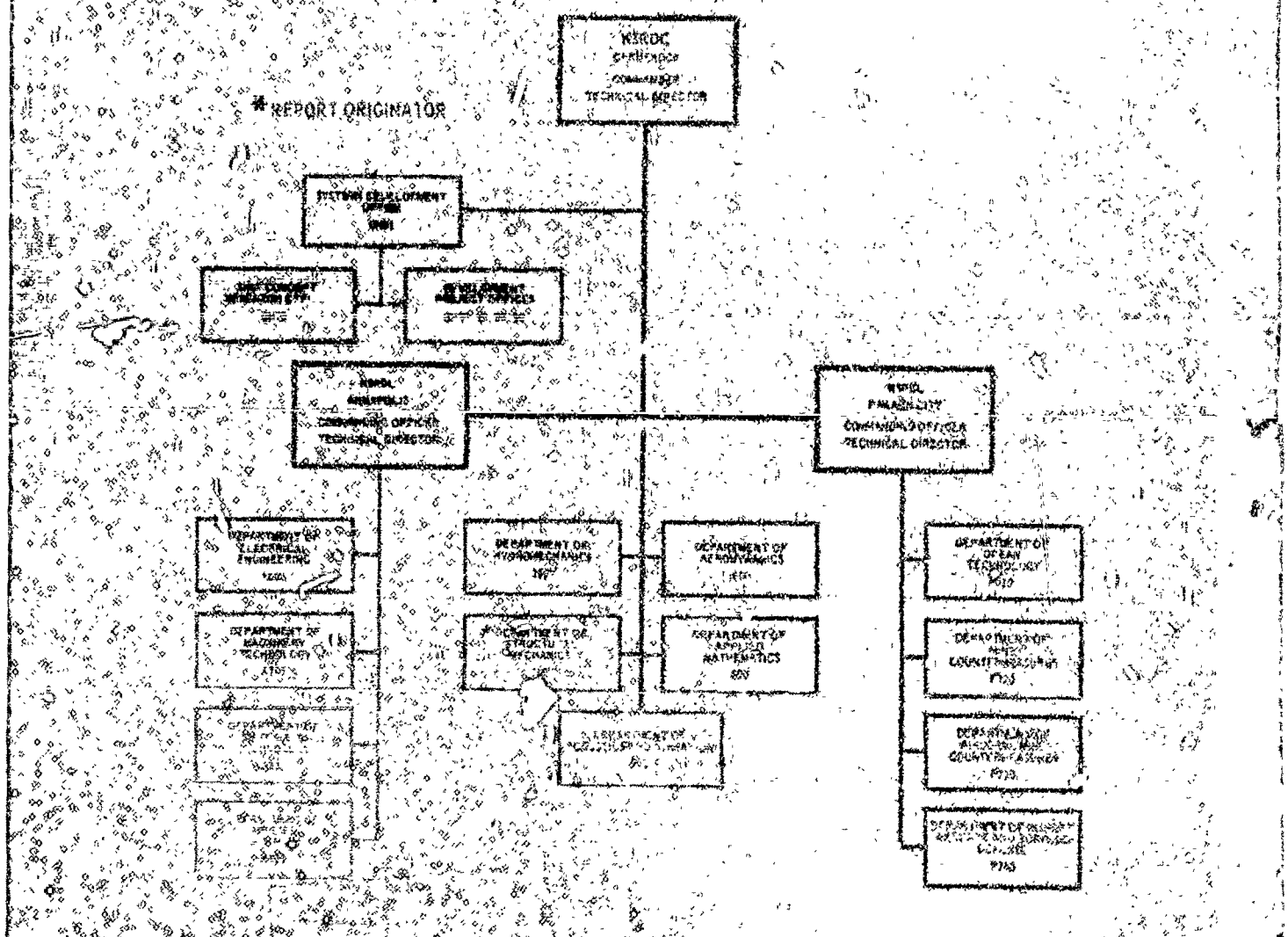

DEPARTMENT OF THE NAVY
NAVAL SHIP RESEARCH AND DEVELOPMENT CENTER
WASHINGTON, D.C. 20034

THE INFLUENCE OF ADDED MASS ON THE NATURAL VIBRATIONS AND IMPULSE RESPONSE OF LONG, THIN CYLINDRICAL SHELLS

by

E. W. Palmer

October 1970

Report 3395

TABLE OF CONTENTS

LIST OF FIGURES

LIST OF TABLES

LIST OF SYMBOLS

A Cross section area of unit width ring.

A_k Mode constants for antisymmetrical branch.

A_{li} Normalized i^{th} mode constant, antisymmetrical branch.

a Radius of neutral surface, or subscript meaning antisymmetrical branch.

a_i Flexural, symmetric, i^{th} mode constant from initial conditions.

a'_i Flexural, symmetric, i^{th} mode constant in terms of a_i.

$\bar{a}_i$ Flexural, antisymmetric, i^{th} mode constant from initial conditions.

a_n Flexural, symmetric, n^{th} mode constant from initial conditions, $R = 0$.

a'_n Flexural, symmetric, n^{th} mode constant from specific initial conditions, $R = 0$.

B_k Mode constants for symmetrical branch.

B_{li} Normalized i^{th} mode constant, symmetrical branch.

b_i Flexural, symmetric, i^{th} mode constant from initial conditions.

$\bar{b}_i$ Flexural, antisymmetric, i^{th} mode constant from initial conditions.

C Frequency parameter, $\frac{ma^2\omega^2}{\bar{E}A}$.

C_e Extensional frequency parameter.

C_f Flexural frequency parameter.

C_M Frequency parameter for case of added mass.

C_m Frequency parameter for case of no added mass.

c Material sound velocity, $\sqrt{\frac{E}{\rho}}$.

c_i Extensional, symmetric, i^{th} mode constant from initial conditions.

$\bar{c}_i$ Extensional, antisymmetric, i^{th} mode constant from initial conditions.

c'_i Extensional, symmetric, i^{th} mode constant in terms of c_i.

c_n Extensional, symmetric, n^{th} mode constant from initial conditions, R = 0.

c'_n Extensional, symmetric, n^{th} mode constant from specific initial conditions, R = 0.

D Determinate of coefficients of constants A_k and B_k.

D_A Determinate of coefficients of constants A_k.

D_B Determinate of coefficients of constants B_k.

D_s Stiffness parameter, $\frac{Eh}{1 - \nu^2}$.

d_i Extensional, symmetric, i^{th} mode constant from initial conditions.

$\bar{d}_i$ Extensional, antisymmetric, i^{th} mode constant from initial conditions.

E Young's modulus.

$\bar{E}$ $\frac{E}{1 - \nu^2}$

E_{ki} Constant in c_i.

e Base of natural logarithms, or subscript meaning extensional class.

F_{ki} Constant in a_i.

f Subscript meaning flexural class.

f_o Rigid body zeroth mode constant.

f_1 Rigid body first mode constant.

G Moment stress resultant.

g_o Rigid body zeroth mode constant.

g_1 Rigid body first mode constant.

h Shell thickness.

h_o Rigid body zeroth mode constant.

h_1 Rigid body first mode constant.

I Moment of inertia of unit width ring cross section about neutral axis.

I_o Maximum impulse amplitude.

i $\sqrt{-1}$, or integer subscript denoting mode number or solution state.

j Integer subscript denoting solution state.

K Stiffness parameter, $\frac{Eh^3}{12(1-\nu^2)}$.

k Integer subscript.

M Mass per unit length of the added line mass.

m Mass per unit length of ring of unit width, or integer subscript.

N Shear stress resultant.

n Integer subscript denoting mode number, R = 0.

n_k Mode parameters from equation (12).

R Mass ratio, $\frac{M}{2\pi ma}$.

r Radial coordinate.

s Subscript meaning symmetrical branch.

T Thrust stress resultant.

t Time variable.

u Axial displacement.

$\ddot{u}$ Axial acceleration.

V Tangential displacement, time independent.

V_i Tangential displacement, time independent, i^{th} mode.

V'_{ia} $\frac{V_i}{A_{1i}}$.

V'_{is} $\frac{V_i}{B_{1i}}$.

v Tangential displacement.

$\ddot{v}$ Tangential acceleration.

v_i Tangential displacement, i^{th} mode.

$\bar{v}$ Initial tangential displacement.

$\dot{v}_i$ Tangential velocity, i^{th} mode.

$\dot{\bar{v}}$ Initial tangential velocity.

W Radial displacement, time independent.

W_i Radial displacement, time independent, i^{th} mode.

W'_{ia} $\frac{W_i}{A_{1i}}$.

W'_{is} $\frac{W_i}{B_{1i}}$.

w Radial displacement.

$\ddot{w}$ Radial acceleration.

w_i Radial displacement, i^{th} mode.

$\bar{w}$ Initial radial displacement.

$\dot{w}_i$ Radial velocity, i^{th} mode.

$\dot{\bar{w}}$ Initial radial velocity.

$\dot{\bar{w}}_o$ Maximum initial radial velocity.

X_{im} Constants in A_{1i}.

Y_{im} Constants in B_{1i}.

Z Stiffness parameter, $\frac{I}{Aa^2}$.

z Axial coordinate.

α_k Circular argument, $n_k \pi$, for coefficients of A_k and B_k.

Γ_n Mode parameter for stress, R = 0.

Γ'_n Mode parameter for stress, R = 0.

θ Angular coordinate.

θ_M Angular location of added mass.

ω Circular frequency of vibration.

ω_i Circular frequency of vibration, i^{th} mode or solution state.

ω_M Circular frequency with added mass.

ω_m Circular frequency, R = 0.

ν Poisson's ratio.

ρ Material mass density.

σ Stress.

σ_G Stress due to moment.

σ_T Stress due to thrust.

τ Non-dimensional time variable, $\frac{ct}{a}$.

ABSTRACT

The plane strain solution is obtained for the natural vibrations and impulse response of a thin circular cylinder containing an added line mass. The solution for a uniform cylinder is derived by taking the added mass to be zero. Numerical calculations of the frequencies and mode shapes for several of the lower modes are presented in graphical form for various values of the added mass. The general impulse response solution for arbitrary initial conditions is obtained by normal mode theory. For both the natural vibrations and impulse response, the theory is found to be in reasonable agreement with available experimental results.

In a particular mode, four distinct solution states are found to exist: a symmetrical and anti-symmetrical branch for each class of vibration, flexural and extensional. Noteworthy features revealed by this investigation are the difference in frequency and mode shape of each solution state and the presence of coupling between the flexural and extensional classes, particularly noticeable in the extensional class mode shapes. In comparing impulse response solutions for velocity with and without the added mass, the major influence of the added mass is found to be an increased participation of the flexural class modes, including the rigid body translation, and decreased participation of the extensional class oscillatory modes.

ADMINISTRATIVE INFORMATION

The research reported herein formed a thesis submitted to and approved by the Graduate Faculty of the Virginia Polytechnic Institute in partial fulfillment of the requirements for the degree of Doctor of Philosophy in Engineering Mechanics.

This report is related to the program entitled "Hull Response Inputs to Equipment," NAVSHIPS Task area SF 35.422.110, Task 15041.

I. INTRODUCTION AND LITERATURE SURVEY

The vibrations of mass loaded cylindrical shells are of interest in many engineering situations; e.g., in the dynamic behavior of hydro and aerospace vehicles with equipment attached to their cylindrical walls. With the added mass considered as an imperfection, such a study should also be important in fundamental studies of vibrations of imperfect bodies of revolution inasmuch as the effect of such imperfections can be quite distinct as has been shown by several experimental investigations [1,2,3]*. A study of the impulse response of such structures is of particular interest in military defense applications, both in response of the shell itself and of attached equipment represented by the added mass.

The first formal analytical work in this area apparently was by Den Hartog [4] in 1928. In studying the natural vibrations of ring-like frames of electrical machines containing lumped masses, he derived approximate fundamental flexural frequencies for these frames by the Rayleigh method. In 1962, Palmer [5] investigated the variations in the natural flexural vibrations without extension due to a lumped mass on a ring by solving the classical eigenvalue problem. A significant result of that study was the difference in frequency and mode shape found between the symmetrical and anti-symmetrical branches of each mode. Michalopoulos and Muster [6] in 1966 obtained the natural vibration solution of a ring-stiffened, mass-loaded cylindrical shell using an energy formulation with the displacements represented approximately by

*Numbers in brackets, [ ], refer to references listed on page 64.

finite Fourier series. The natural vibrations of a stiffened pressurized cylindrical shell with an attached mass were considered by Ojalvo and Newman [7] in 1967 by an approximate energy technique. They determined mode shapes for the shell without the attached mass and used these as assumed mode shapes to determine the natural vibrations for the shell-mass system. Lee, et al, [8] in 1968 analyzed the natural vibrations of mass-loaded ring structures by two approximate methods, finite-element and transfer matrix. Using essentially the same approach as Michalopoulos and Muster, Lee, et al, also studied the natural vibrations of mass-loaded shell structures. Although the natural vibrations of mass-loaded beam and plate structures are well established, e.g., Thornton [9], a literature search has failed to reveal a complete rigorous solution for the natural vibrations of mass-loaded ring and cylindrical shell structures.

Previous solution attempts to the subject problem can, with one exception [5], be characterized by the approach used by Ojalvo and Newman [7], in which the mode shapes for the uniform shell without added mass were used as trial functions in an energy formulation for the solution of the complete shell-mass system. A rigorous solution as presented herein is desirable since it is well known that even crude trial functions used in an energy formulation can give quite good results for the natural frequencies, at least for the lower modes, but mode shapes, and response parameters computed from them for a specified problem, may be subject to question.

The problem of impulse response of a mass-loaded cylindrical shell has been treated by Michalopoulos and Muster [6]. They used modal

analysis to formulate the response of the structure to a band of uniform internal pressure applied as a pulse in time. However, numerical results were not presented. With the above exception, the impulse response of mass-loaded shell structures apparently has not been treated in the literature. The simpler, degenerate problem of the response of uniform thin rings and cylinders to non-moving impulse loads has, however, received some attention. Palmer [10] used modal analysis to obtain the response of a ring to a side pressure pulse represented as an initial velocity distribution. In that study, the effects of flexure and extension were completely uncoupled. Humphreys and Winter [11] employed the Laplace transform approach to solve slightly simplified thin shell equations for an infinitely long cylinder under a transverse pressure pulse. Sheng [12] solved Donnell-type shell equations for the response of a cylindrical shell to a semisinusoidal surface pulse. Johnson and Greif [13] used two different numerical methods of timewise integration to obtain the response of a cylindrical shell to a blast loading. Their solution was completely numerical and involved expressing Sanders' shell equations in finite difference form.

II. STATEMENT OF THE PROBLEM

The plane strain solution for the natural vibrations and impulse response of infinitely long, thin circular cylindrical shells containing an added concentrated line mass will be obtained. The shell material will be isotropic, homogenous and the analysis will employ linearized, small deformation, thin shell theory neglecting the effects of shear deformation and rotatory inertia, as formulated by Flugge [14].

The midsurface displacements u, v, and w and the coordinate system for the shell are defined in Figure 1. The line mass, M, is concentrated at the midsurface and is parallel to the z-axis. Rotatory inertia of the concentrated mass is neglected. Motion will occur only in planes perpendicular to the z-axis.

The solution for the natural frequencies and mode shapes will be obtained in the classical manner by describing continuity and equilibrium conditions at the mass. The influence of the mass will be ascertained by comparison with the vibrations of a cylinder without added mass. The exact solution to the governing equations will be obtained for both extensional and flexural classes of vibration with no approximations made on either class. In a previous solution by Palmer [5] only the flexural class was considered in an approximate manner, i.e., flexure with the midsurface extension everywhere zero, or $w = \frac{\partial v}{\partial \theta}$. The analytical frequencies will be compared with those obtained experimentally by Lee [8].

The solution for the natural vibrations will be used to determine the response of the shell to a transverse impulse. The impulse will be specified in terms of initial conditions on the displacements and

velocities, and then the mode constants will be determined through the orthogonality relation. The influence of the mass will be determined by comparing the response with and without the mass. As noted in the literature review, Palmer [10] obtained the response without the added mass to an initial velocity distribution by modal analysis. Although both extensional and flexural classes were considered, that solution was an approximation since extension was assumed to occur without flexure and flexure without extension. Such simplifications permitted a solution to be obtained in a relatively straightforward manner. The impulse response solution will be compared with experimental results of Navy tests, reported in [15] and [20], and Sandia Corporation tests [16].

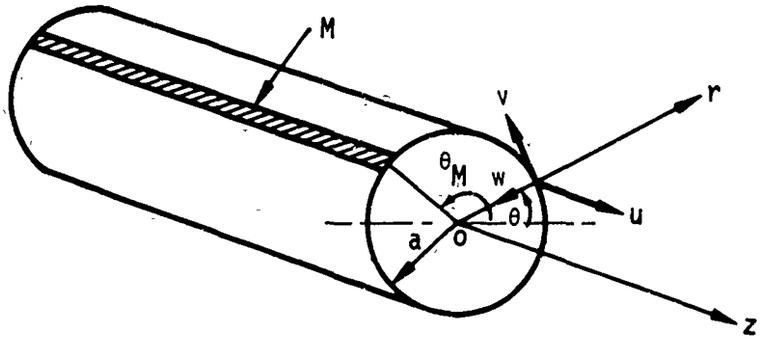

Figure 1 - Coordinate System

III. NATURAL VIBRATIONS

The general solution will be obtained for the natural frequencies and normal mode shapes. Numerical calculations of the frequencies and mode shapes for several of the lower modes will be presented in graphical form and compared with experimental results [8].

A. Governing Equations

The complete thin cylindrical shell theory equations of motion presented by Flugge [14], using the coordinate system of Figure 1, adding inertia terms and omitting load terms for natural vibrations, are

$$u_{zz} + \frac{1-\nu}{2}u_{00} + \frac{1+\nu}{2}v_{0z} - \nu w_z + \frac{K}{D_s a^2}\left[\frac{1-\nu}{2}u_{00} + w_{zzz} - \frac{1-\nu}{2}w_{00z}\right] - \frac{m\ddot{u}a^2}{D_s} = 0 \qquad (1)$$

$$\frac{1+\nu}{2}u_{0z} + v_{00} + \frac{1-\nu}{2}v_{zz} + \frac{K}{D_s a^2}\left[\frac{3}{2}(1-\nu)v_{zz} + \frac{3-\nu}{2}w_{0zz}\right] - w_0 - \frac{m\ddot{v}a^2}{D_s} = 0 \qquad (2)$$

$$\nu u_z + v_0 - w + \frac{K}{D_s a^2}\left[\frac{1-\nu}{2}u_{00z} - u_{zzz} - \frac{3-\nu}{2}v_{0zz} - w_{zzzz} - 2w_{00zz} - w_{0000} - 2w_{00} - w\right] - \frac{m\ddot{w}a^2}{D_s} = 0 \qquad (3)$$

For the case of plane strain, $u = 0$ and $(\,)_z = 0$, these three equations reduce to two in the planar displacement components v and w. Thus

$$-\frac{ma^2\ddot{v}}{D_s} + v_{00} - w_0 = 0 \qquad (4)$$

$$-\frac{ma^2\ddot{w}}{D_s} + v_0 - w - \frac{K}{D_s a^2}\left[w_{0000} + 2w_{00} + w\right] = 0 \qquad (5)$$

where

$$(\,)_0 = \frac{\partial(\,)}{\partial\theta}$$

and

$$\dot{(\,)} = \frac{\partial(\,)}{\partial t}$$

Since it is desired to treat rings as well as stiffened cylinders, it is convenient to change the form of the stiffness parameters D_s and K for a ring of unit width as follows:

$$D_s = \frac{Eh}{1-\nu^2} = \bar{E}h = \bar{E}A$$

and

$$\frac{K}{D_s a^2} = \frac{1}{D_s a^2}\left[\frac{Eh^3}{12(1-\nu^2)}\right] = \frac{I}{Aa^2}$$

With these substitutions, equations (4) and (5) can be written in the form

$$-\text{maw} + \frac{EA}{a}(v_\theta - w_\theta) = 0 \tag{6}$$

$$-\text{maw} + \frac{EA}{a}(v_\theta - w) - \frac{\bar{E}I}{a^3}(w_{\theta\theta\theta\theta} + 2w_{\theta\theta} + w) = 0 \tag{7}$$

It is noted that equations (6) and (7) also were derived by Baron and Bleich [17].

B. Solution of the Governing Equations

Suitable solutions to equations (6) and (7) for harmonic vibrations are, for a particular mode,

$$v = V(\theta)\, e^{i\omega t} \tag{8}$$

and

$$w = W(\theta)\, e^{i\omega t} \tag{9}$$

where

$$V(\theta) = \sum_{k=1}^{3} n_k \left(A_k \cos n_k\theta + B_k \sin n_k\theta\right) \tag{10}$$

and

$$W(\theta) = \sum_{k=1}^{3} \left(\frac{ma^2\omega^2}{\bar{E}A} - n_k^2\right)\left(A_k \sin n_k\theta - B_k \cos n_k\theta\right) \tag{11}$$

Substituting (8) and (9) into (6) and (7), it is found that equation (6) is identically satisfied, whereas equation (7) will be

satisfied if the following relation is in turn satisfied:

$$C^2 - \left[(n^2-1)^2 Z + n^2 + 1\right] C + n^2 (n^2 - 1)^2 Z = 0 \tag{12}$$

where

$$C = \frac{ma^2\omega^2}{\bar{E}A} \tag{13}$$

and

$$Z = \frac{I}{Aa^2} \tag{14}$$

The n_1, n_2, and n_3 of equations (10) and (11), are roots of equation (12), which is cubic in n^2. As expected, equation (12), the frequency equation, is quadratic in the frequency parameter C. It will be shown shortly that for a given value of n the lesser value of C represents primarily flexural vibration and the greater value represents primarily extensional, or membrane, vibration.

C. Consideration of the Added Mass

As the solutions (10) and (11) contain six constants of integration, A_k and B_k, at least one always remaining arbitrary since (6) and (7) are homogeneous, and since the frequency parameter C must also be determined, then six relations are needed at the added mass.

From continuity conditions, the following equations can be written

$$\left[v\right]_{-\theta_M}^{\theta_M} = v(\theta_M) - v(-\theta_M) = 0 \tag{15}$$

$$\left[w\right]_{-\theta_M}^{\theta_M} = 0 \tag{16}$$

$$\left[w_\theta\right]_{-\theta_M}^{\theta_M} = 0 \tag{17}$$

From equilibrium, see Figure 2, summing forces in the radial direction gives

$$M\ddot{w}(\theta_M) + \left[N\right]_{-\theta_M}^{\theta_M} = 0 \tag{18}$$

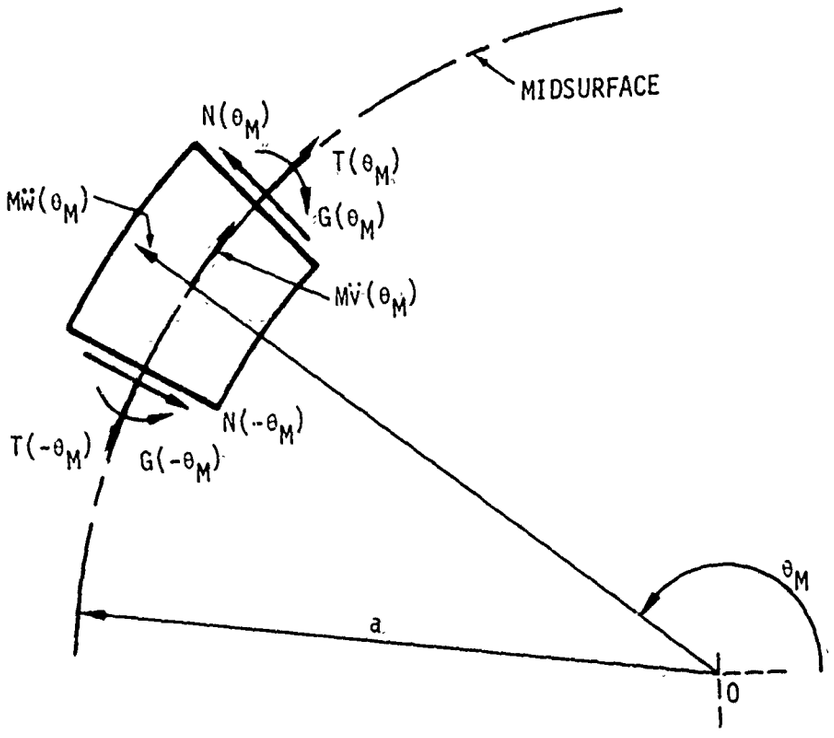

Figure 2 - Dynamical Equilibrium of the Added Mass

and in the tangential direction gives

$$M\ddot{v}(\theta_M) + \left[T\right]_{-\theta_M}^{\theta_M} = 0 \tag{19}$$

and summing the moments gives

$$\left[G\right]_{-\theta_M}^{\theta_M} = 0 \tag{20}$$

where N, T, and G are the respective shear, thrust and moment stress resultants. From Flugge [14], with present notation, these are

$$N = -\frac{\bar{E}I}{a^3}(w_{000} + w_0) \tag{21}$$

$$T = \frac{\bar{E}A}{a}(v_0 - w) - \frac{\bar{E}I}{a^3}(w + w_{00}) \tag{22}$$

$$G = \frac{\bar{E}I}{a^2}(w + w_{00}) \tag{23}$$

Evaluating (15) through (20) with expressions (8), (9), (21), (22), and (23) gives six linear homogeneous algebraic equations arranged as follows:

from (16)

$$\sum_{k=1}^{3} A_k (C - n_k^2) \sin \alpha_k = 0 \tag{24}$$

from (20)

$$\sum_{k=1}^{3} A_k n_k^2 (C - n_k^2) \sin \alpha_k = 0 \tag{25}$$

from (19)

$$\sum_{k=1}^{3} A_k n_k (\pi RC \cos \alpha_k + n_k \sin \alpha_k) = 0 \tag{26}$$

from (15)

$$\sum_{k=1}^{3} B_k n_k \sin \alpha_k = 0 \tag{27}$$

from (17)

$$\sum_{k=1}^{3} B_k n_k^3 \sin \alpha_k = 0 \tag{28}$$

and from (18)

$$\sum_{k=1}^{3} B_k \left[\pi R \frac{C}{Z} (C - n_k^2) \cos \alpha_k - n_k^5 \sin \alpha_k \right] = 0 \tag{29}$$

where $R = \frac{M}{2\pi a m}$, the mass ratio, (30)

and $\alpha_k = n_k \theta_M$, $k = 1, 2, \text{or } 3$. (31)

Without any loss of generality, θ_M will be taken as π for the remainder of this dissertation.

D. Natural Frequencies

Since (24) through (29) are homogeneous, the determinant of the coefficients of the A_k and B_k terms must vanish in order for non-trivial values of these constants to exist.

The sixth order determinant formed from (24) through (29) is

$$D = \begin{vmatrix} D_A & O \\ O & D_B \end{vmatrix} = 0 \tag{32}$$

where

$$D_A = \begin{vmatrix} (C - n_1^2)\sin\alpha_1 & (C - n_2^2)\sin\alpha_2 & (C - n_3^2)\sin\alpha_3 \\ n_1^2(C - n_1^2)\sin\alpha_1 & n_2^2(C - n_2^2)\sin\alpha_2 & n_3^2(C - n_3^2)\sin\alpha_3 \\ n_1(\pi RC\cos\alpha_1 + n_1\sin\alpha_1) & n_2(\pi RC\cos\alpha_2 + n_2\sin\alpha_2) & n_3(\pi RC\cos\alpha_3 + n_3\sin\alpha_3) \end{vmatrix} \tag{33}$$

and

$$D_B = \begin{vmatrix} n_1\sin\alpha_1 & n_2\sin\alpha_2 & n_3\sin\alpha_3 \\ n_1^3\sin\alpha_1 & n_2^3\sin\alpha_2 & n_3^3\sin\alpha_3 \\ \pi R\frac{C}{Z}(C - n_1^2)\cos\alpha_1 - n_1^5\sin\alpha_1 & \pi R\frac{C}{Z}(C - n_2^2)\cos\alpha_2 - n_2^5\sin\alpha_2 & \pi R\frac{C}{Z}(C - n_3^2)\cos\alpha_3 - n_3^5\sin\alpha_3 \end{vmatrix} \tag{34}$$

Equation (32) is expressed as a product of two third-order determinants, one containing only coefficients of A_k and the other containing only coefficients of B_k. Thus

$$D = D_A D_B = 0 \tag{35}$$

Equation (35) may be satisfied in three ways

$$D_A = 0 \tag{36}$$

$$D_B = 0 \tag{37}$$

or

$$D_A = D_B = 0 \tag{38}$$

In the first of these, (36), nontrivial values are possible for the A_k constants since $D_A = 0$. But if $D_A = 0$ and $D_B \neq 0$, then all the B_k constants will be zero, since by Cramer's rule nontrivial

values cannot exist. The reverse is true for the second of these, (37). Referring to the expression for the radial displacement function, (11), we find that the A_k constants are associated with sine functions which are antisymmetrical, whereas the B_k constants are associated with symmetrical cosine functions. Condition (36) then would result in a solution containing only antisymmetrical terms and the solution from (37) would contain only symmetrical terms.

In either case, (36) or (37), both the governing equations and the continuity and equilibrium conditions at the mass will be satisfied.

The frequency equations may be found by evaluating D_A and D_B. From (33)

$$\begin{aligned} D_A = {} & n_1^2 n_2 (C - n_1^2)(C - n_2^2) \sin a_1 \sin a_3 (\pi RC \cos a_2 + n_2 \sin a_2) \\ & + n_2^2 n_3 (C - n_1^2)(C - n_2^2) \sin a_1 \sin a_2 (\pi RC \cos a_3 + n_3 \sin a_3) \\ & + n_3^2 n_1 (C - n_2^2)(C - n_3^2) \sin a_2 \sin a_3 (\pi RC \cos a_1 + n_1 \sin a_1) \\ & - n_1 n_2^2 (C - n_2^2)(C - n_3^2) \sin a_2 \sin a_3 (\pi RC \cos a_1 + n_1 \sin a_1) \\ & - n_2 n_3^2 (C - n_1^2)(C - n_3^2) \sin a_1 \sin a_3 (\pi RC \cos a_2 + n_2 \sin a_2) \\ & - n_3 n_1^2 (C - n_1^2)(C - n_2^2) \sin a_1 \sin a_2 (\pi RC \cos a_3 + n_3 \sin a_3) \end{aligned} \tag{39}$$

Setting $D_A = 0$ the frequency equation for antisymmetrical vibrations is obtained. Solving this expression for the mass ratio and letting $R = R_A$ for $D_A = 0$ gives

$$\begin{aligned} R_A = {} & \Big[n_1^2 (C - n_2^2)(C - n_3^2)(n_2^2 - n_3^2) + n_2^2 (C - n_1^2)(C - n_3^2)(n_3^2 - n_1^2) \\ & + n_3^2 (C - n_1^2)(C - n_2^2)(n_1^2 - n_2^2) \Big] \div \pi C \left[n_1 (C - n_2^2)(C - n_3^2)(n_3^2 - n_2^2) \frac{\cos a_1}{\sin a_1} \right. \\ & \left. + n_2 (C - n_1^2)(C - n_3^2)(n_1^2 - n_3^2) \frac{\cos a_2}{\sin a_2} + n_3 (C - n_1^2)(C - n_2^2)(n_2^2 - n_1^2) \frac{\cos a_3}{\sin a_3} \right] \end{aligned} \tag{40}$$

By the same procedure, we find from (37)

$$D_B = n_1 n_2 n_3 \left[n_2^2 n_3^2 (n_2^2 - n_3^2) + n_1^2 n_2^2 (n_1^2 - n_2^2) + n_1^2 n_3^2 (n_3^2 - n_1^2) \right]$$
$$+ \pi R \frac{C}{Z} \left[n_1 n_2 (n_2^2 - n_1^2)(C - n_3^2) \frac{\cos a_3}{\sin a_3} + n_2 n_3 (n_3^2 - n_2^2)(C - n_1^2) \frac{\cos a_1}{\sin a_1} \right.$$
$$\left. + n_1 n_3 (n_1^2 - n_3^2)(C - n_2^2) \frac{\cos a_2}{\sin a_2} \right] \qquad (41)$$

from which the mass ratio for symmetrical vibrations, R_B , is

$$R_B = n_1 n_2 n_3 \left[n_2^2 n_3^2 (n_3^2 - n_2^2) + n_1^2 n_2^2 (n_2^2 - n_1^2) + n_1^2 n_3^2 (n_1^2 - n_3^2) \right]$$
$$\div \pi \frac{C}{Z} \left[n_2 n_3 (n_3^2 - n_2^2)(C - n_1^2) \frac{\cos a_1}{\sin a_1} + n_1 n_3 (n_1^2 - n_3^2)(C - n_2^2) \frac{\cos a_2}{\sin a_2} \right.$$
$$\left. + n_1 n_2 (n_2^2 - n_1^2)(C - n_3^2) \frac{\cos a_3}{\sin a_3} \right] \qquad (42)$$

In general, both D_A and D_B will not vanish for the same n_k , C and R values since expressions (40) and (42) are not the same. Now referring to equations (12), (40), and (42), it is apparent that for natural vibrations with an added mass four solutions are possible; one consisting of symmetrical vibrations and another of antisymmetrical vibrations for each of the two classes, flexural and extensional. An illustration of this is provided in the next section where numerical solutions are obtained.

The frequency equation for the case of a uniform cylinder or ring may be obtained by letting the mass ratio become zero in (40) and (42). From (40), multiplying through by $\sin a_1 \sin a_2 \sin a_3$,

$$\left[n_1^2 (C - n_2^2)(C - n_3^2)(n_2^2 - n_3^2) + n_2^2 (C - n_1^2)(C - n_3^2)(n_3^2 - n_1^2) \right.$$
$$\left. + n_3^2 (C - n_1^2)(C - n_2^2)(n_1^2 - n_2^2) \right] \sin a_1 \sin a_2 \sin a_3 = 0 \qquad (43)$$

and from (42), again multiplying by $\sin a_1 \sin a_2 \sin a_3$,

$$n_1 n_2 n_3 \left[n_2^2 n_3^2 (n_3^2 - n_2^2) + n_1^2 n_2^2 (n_2^2 - n_1^2) \right.$$
$$\left. + n_1^2 n_3^2 (n_1^2 - n_3^2) \right] \sin a_1 \sin a_2 \sin a_3 = 0 \qquad (44)$$

In this case, with $\theta_M = \pi$, if one of the n_k is an integer, then (43) or (44) will be satisfied. Actually, for this situation, both (43) and (44) are identically zero, which is condition (38). Then equation (12) suffices as the frequency equation, with one of the n_k an integer.

E. Normal Mode Shapes

The antisymmetrical branch mode constants A_k may be found by solving (24) and (25) simultaneously; the solution is

$$\frac{A_2}{A_1} = \frac{(n_3^2 - n_1^2)(C - n_1^2)\sin a_1}{(n_2^2 - n_3^2)(C - n_2^2)\sin a_2} \tag{45}$$

and

$$\frac{A_3}{A_1} = \frac{(n_1^2 - n_2^2)(C - n_1^2)\sin a_1}{(n_2^2 - n_3^2)(C - n_3^2)\sin a_3} \tag{46}$$

and the symmetrical constants B_k from (27) and (28) are

$$\frac{B_2}{B_1} = \frac{n_1 (n_3^2 - n_1^2)\sin a_1}{n_2 (n_2^2 - n_3^2)\sin a_2} \tag{47}$$

and

$$\frac{B_3}{B_1} = \frac{n_1 (n_1^2 - n_2^2)\sin a_1}{n_3 (n_2^2 - n_3^2)\sin a_3} \tag{48}$$

where A_1 and B_1 are arbitrary. From (10) and (11) the tangential and radial displacement functions for the antisymmetrical branch are

$$V = A_1 \left[n_1 \cos n_1\theta + \frac{A_2}{A_1} n_2 \cos n_2\theta + \frac{A_3}{A_1} n_3 \cos n_3\theta \right] \tag{49}$$

and

$$W = A_1 \left[(C - n_1^2)\sin n_1\theta + \frac{A_2}{A_1}(C - n_2^2)\sin n_2\theta + \frac{A_3}{A_1}(C - n_3^2)\sin n_3\theta \right] \tag{50}$$

and for the symmetrical branch are

$$V = B_1 \left[n_1 \sin n_1\theta + \frac{B_2}{B_1} n_2 \sin n_2\theta + \frac{B_3}{B_1} n_3 \sin n_3\theta \right] \tag{51}$$

and

$$W = B_1 \left[(n_1^2 - C) \cos n_1\theta + \frac{B_2}{B_1} (n_2^2 - C) \cos n_2\theta + \frac{B_3}{B_1} (n_3^2 - C) \cos n_3\theta \right] \tag{52}$$

With n_1 an integer, then (45) through (48) are zero and the mode shapes without the added mass are for antisymmetrical vibrations

$$V = A_1 n_1 \cos n_1\theta \tag{53}$$

and

$$W = A_1 (C - n_1^2) \sin n_1\theta \tag{54}$$

and for symmetrical vibrations

$$V = B_1 n_1 \sin n_1\theta \tag{55}$$

and

$$W = B_1 (n_1^2 - C) \cos n_1\theta \tag{56}$$

In modal analysis problems where the orthogonality condition must be used to obtain a solution, it is convenient to normalize the mode shapes. The orthogonality condition between the modes, from Love [18], can be written as

$$(\omega_i^2 - \omega_j^2) \left\{ m \int_{-\pi}^{\pi} (V_i V_j + W_i W_j)\, a d\theta + M (V_i V_j + W_i W_j)_{\pi} \right\} = 0 \tag{57}$$

where i and j are indices representing two solution states, or normal modes, with corresponding frequencies ω_i and ω_j. If $\omega_i \neq \omega_j$, then the bracketed quantity of (57) must vanish, and if $\omega_i = \omega_j$, (57)

is identically satisfied. In the latter situation, the value of the bracketed quantity is then arbitrary. However, it is customary to normalize this term by making its value some convenient quantity. For the case of i = j, the bracketed quantity of (57) can be taken as

$$m\int_{-\pi}^{\pi}\left[V_i^2+W_i^2\right]ad\theta+M\left[V_i^2+W_i^2\right]_{\pi}=2\pi ma \tag{58}$$

Dividing (58) by $2\pi ma$, we have

$$\frac{1}{2\pi}\int_{-\pi}^{\pi}\left[V_i^2+W_i^2\right]d\theta+R\left[V_i^2+W_i^2\right]_{\pi}=1 \tag{59}$$

With equations (49) and (50) written as

$$V_i=A_{1i}V'_{ia} \text{ and } W_{ai}=A_{1i}W'_{ia} \tag{60}$$

for the i^{th} mode, and substituting (60) into (59) and solving for A_{1i}, we have

$$A_{1i}^2=\frac{1}{\frac{1}{2\pi}\int_{-\pi}^{\pi}\left[V_{ia}'^2+W_{ia}'^2\right]d\theta+R\left[V_{ia}'^2+W_{ia}'^2\right]_{\pi}} \tag{61}$$

Similarly, for B_{1i} we obtain

$$B_{1i}^2=\frac{1}{\frac{1}{2\pi}\int_{-\pi}^{\pi}\left[V_{is}'^2+W_{is}'^2\right]d\theta+R\left[V_{is}'^2+W_{is}'^2\right]_{\pi}} \tag{62}$$

where the indices a and s represent the antisymmetrical and symmetrical branches respectively.

Evaluating the integrals of (61) and (62) is a straightforward but somewhat lengthy process. The resulting expressions are as follows:

$$A_{1i}^2=\frac{1}{\frac{1}{2\pi}\sum_{m=1}^{12}X_{im}+R\left[V_{ia}'^2+W_{ia}'^2\right]_{\pi}} \tag{63}$$

where the X_{im} are

$$X_{i1} = (C_{ia} - n_{1ia}^2)^2\left[\pi - \frac{\sin 2n_{1ia}\pi}{2n_{1ia}}\right] \tag{64}$$

$$X_{i2} = \left(\frac{A_2}{A_1}\right)^2(C_{ia} - n_{2ia}^2)^2\left[\pi - \frac{\sin 2n_{2ia}\pi}{2n_{2ia}}\right] \tag{65}$$

$$X_{i3} = \left(\frac{A_3}{A_1}\right)^2(C_{ia} - n_{3ia}^2)^2\left[\pi - \frac{\sin 2n_{3ia}\pi}{2n_{3ia}}\right] \tag{66}$$

$$X_{i4} = 2\left(\frac{A_2}{A_1}\right)(C_{ia} - n_{1ia}^2)(C_{ia} - n_{2ia}^2)\left[\frac{\sin (n_{1ia} - n_{2ia})\pi}{n_{1ia} - n_{2ia}} - \frac{\sin (n_{1ia} + n_{2ia})\pi}{n_{1ia} + n_{2ia}}\right] \tag{67}$$

$$X_{i5} = 2\left(\frac{A_3}{A_1}\right)(C_{ia} - n_{1ia}^2)(C_{ia} - n_{3ia}^2)\left[\frac{\sin (n_{1ia} - n_{3ia})\pi}{n_{1ia} - n_{3ia}} - \frac{\sin (n_{1ia} + n_{3ia})\pi}{n_{1ia} + n_{3ia}}\right] \tag{68}$$

$$X_{i6} = 2\left(\frac{A_2}{A_1}\right)\left(\frac{A_3}{A_1}\right)(C_{ia} - n_{2ia}^2)(C_{ia} - n_{3ia}^2)\left[\frac{\sin (n_{2ia} - n_{3ia})\pi}{n_{2ia} - n_{3ia}} - \frac{\sin (n_{2ia} + n_{3ia})\pi}{n_{2ia} + n_{3ia}}\right] \tag{69}$$

$$X_{i7} = n_{1ia}^2\left[\pi + \frac{\sin 2n_{1ia}\pi}{2n_{1ia}}\right] \tag{70}$$

$$X_{i8} = \left(\frac{A_2}{A_1}\right)^2 n_{2ia}^2\left[\pi + \frac{\sin 2n_{2ia}\pi}{2n_{2ia}}\right] \tag{71}$$

$$X_{i9} = \left(\frac{A_3}{A_1}\right)^2 n_{3ia}^2\left[\pi + \frac{\sin 2n_{3ia}\pi}{2n_{3ia}}\right] \tag{72}$$

$$X_{i10} = 2\left(\frac{A_2}{A_1}\right)n_{1ia}n_{2ia}\left[\frac{\sin (n_{1ia} - n_{2ia})\pi}{n_{1ia} - n_{2ia}} + \frac{\sin (n_{1ia} + n_{2ia})\pi}{n_{1ia} + n_{2ia}}\right] \tag{73}$$

$$X_{i11} = 2\left(\frac{A_3}{A_1}\right)n_{1ia}n_{3ia}\left[\frac{\sin (n_{1ia} - n_{3ia})\pi}{n_{1ia} - n_{3ia}} + \frac{\sin (n_{1ia} + n_{3ia})\pi}{n_{1ia} + n_{3ia}}\right] \tag{74}$$

$$X_{i12} = 2\left(\frac{A_2}{A_1}\right)\left(\frac{A_3}{A_1}\right)n_{2ia}n_{3ia}\left[\frac{\sin (n_{2ia} - n_{3ia})\pi}{n_{2ia} - n_{3ia}} + \frac{\sin (n_{2ia} + n_{3ia})\pi}{n_{2ia} + n_{3ia}}\right] \tag{75}$$

and $$B_{1i}^2 = \frac{1}{\frac{1}{2\pi}\sum_{m=1}^{12} Y_{im} + R\left[V_{is}'^2 + W_{is}'^2\right]_\pi} \tag{76}$$

where the Y_{im} are

$$Y_{i1} = (n_{1is}^2 - C_{is})^2\left[\pi + \frac{\sin 2n_{1is}\pi}{2n_{1is}}\right] \tag{77}$$

$$Y_{i2} = \left(\frac{B_2}{B_1}\right)^2 (n_{2is}^2 - C_{is})^2\left[\pi + \frac{\sin 2n_{2is}\pi}{2n_{2is}}\right] \tag{78}$$

$$Y_{i3} = \left(\frac{B_3}{B_1}\right)^2 (n_{3is}^2 - C_{is})^2\left[\pi + \frac{\sin 2n_{3is}\pi}{2n_{3is}}\right] \tag{79}$$

$$Y_{i4} = 2\left(\frac{B_2}{B_1}\right)(n_{1is}^2 - C_{is})(n_{2is}^2 - C_{is})\left[\frac{\sin (n_{1is} - n_{2is})\pi}{n_{1is} - n_{2is}} + \frac{\sin (n_{1is} + n_{2is})\pi}{n_{1is} + n_{2is}}\right] \tag{80}$$

$$Y_{i5} = 2\left(\frac{B_3}{B_1}\right)(n_{1is}^2 - C_{is})(n_{3is}^2 - C_{is})\left[\frac{\sin (n_{1is} - n_{3is})\pi}{n_{1is} - n_{3is}} + \frac{\sin (n_{1is} + n_{3is})\pi}{n_{1is} + n_{3is}}\right] \tag{81}$$

$$Y_{i6} = 2\left(\frac{B_2}{B_1}\right)\left(\frac{B_3}{B_1}\right)(n_{2is}^2 - C_{is})(n_{3is}^2 - C_{is})\left[\frac{\sin (n_{2is} - n_{3is})\pi}{n_{2is} - n_{3is}} + \frac{\sin (n_{2is} + n_{3is})\pi}{n_{2is} + n_{3is}}\right] \tag{82}$$

$$Y_{i7} = n_{1is}^2\left[\pi - \frac{\sin 2n_{1is}\pi}{2n_{1is}}\right] \tag{83}$$

$$Y_{i8} = \left(\frac{B_2}{B_1}\right)^2 n_{2is}^2\left[\pi - \frac{\sin 2n_{2is}\pi}{2n_{2is}}\right] \tag{84}$$

$$Y_{i9} = \left(\frac{B_3}{B_1}\right)^2 n_{3is}^2\left[\pi - \frac{\sin 2n_{3is}\pi}{2n_{3is}}\right] \tag{85}$$

$$Y_{i10} = 2\left(\frac{B_2}{B_1}\right) n_{1is} n_{2is}\left[\frac{\sin (n_{1is} - n_{2is})\pi}{n_{1is} - n_{2is}} - \frac{\sin (n_{1is} + n_{2is})\pi}{n_{1is} + n_{2is}}\right] \tag{86}$$

$$Y_{i11} = 2\left(\frac{B_3}{B_1}\right) n_{1is} n_{3is}\left[\frac{\sin (n_{1is} - n_{3is})\pi}{n_{1is} - n_{3is}} - \frac{\sin (n_{1is} + n_{3is})\pi}{n_{1is} + n_{3is}}\right] \tag{87}$$

$$Y_{i12} = 2\left(\frac{B_2}{B_1}\right)\left(\frac{B_3}{B_1}\right) n_{2is} n_{3is}\left[\frac{\sin (n_{2is} - n_{3is})\pi}{n_{2is} - n_{3is}} - \frac{\sin (n_{2is} + n_{3is})\pi}{n_{2is} + n_{3is}}\right] \tag{88}$$

F. Numerical Solutions

To illustrate the influence of the added mass, frequencies and mode shapes were calculated for several of the lower modes by the following procedure:

1. Influence of Mass on Frequencies

a. After selecting a value of the stiffness parameter Z, values of n_1 were chosen and (12) was solved for the flexural frequency parameters C_f and the extensional frequency parameters C_e. Then for each frequency parameter, C_f and C_e, (12) was solved again for the modal parameters n_{2f} and n_{3f} for the flexural class, and n_{2e} and n_{3e} for the extensional class. Integer values of n_1 will give solutions for the problem without the added mass.

b. The n_k and C values were then inserted into equations (40) and (42) to determine values of the mass ratio, R. Note that for each n_1 chosen, four values of R will be obtained, R_{fa}, R_{fs}, R_{ea} and R_{es}, where f corresponds to flexure, e to extension, a to antisymmetric and s to symmetric.

c. Frequency ratios of the structure with added mass to that without added mass were obtained from equation (13):

$$\frac{\omega_M}{\omega_m} = \left(\frac{C_M}{C_m}\right)^{1/2} \tag{89}$$

For several individual lower modes, the above parameters were calculated and are given in Tables 1 and 2. The relationship between frequency and mass is also shown graphically in Figures 3 through 6.

TABLE 1 - NATURAL FREQUENCIES, EXTENSIONAL CLASS, Z = 0.0001

n_1	C	n_2	n_3	$\frac{\omega_M}{\omega_m}$	R_{ea}	R_{es}
			ZEROTH MODE			
0.0	1.000100	9.924777i	10.074785	1.0	0.0	0.0
0.093543i	0.991352	9.902667i	10.053005	0.996	--	0.10
0.096365i	0.990817	9.901308i	10.051667	0.995	--	1.0
0.096652i	0.990761	9.901168i	10.051528	0.995	--	10.0
			FIRST MODE			
1.0	2.0	11.828873i	11.955009	1.0	0.0	0.0
0.920444	1.847218	11.593651i	11.722319	0.962	0.086	0.10
0.909462	1.827122	11.561633i	11.690650	0.956	0.10	0.178
0.895314	1.801590	11.520569i	11.650043	0.950	0.118	1.0
0.892210	1.796041	11.511586i	11.461161	0.948	0.123	10.0
0.685508	1.469940	10.942573i	11.078805	0.858	1.0	--
0.668459	1.446858	10.898814i	11.035586	0.852	10.0	--
			SECOND MODE			
2.0	5.000180	14.903623i	15.003939	1.0	0.0	0.0
1.923135	4.698604	14.672060i	14.773947	0.970	0.04	0.10
1.905064	4.629420	14.617369i	14.719634	0.962	0.051	1.0
1.902883	4.621112	14.610760i	14.713071	0.961	0.052	10.0
1.832289	4.357412	14.396191i	14.500016	0.934	0.10	--
1.673354	3.800200	13.908495i	14.015931	0.872	1.0	--
1.671937	3.795457	13.904119i	14.011589	0.871	10.0	--

TABLE 2 - NATURAL FREQUENCIES, FLEXURAL CLASS, Z = 0.0001

n_1	C	n_2	n_3	$\frac{\omega_M}{\omega_m}$	R_{fa}	R_{fs}
			SECOND MODE			
		(n_2 = a+bi, n_3 = a-bi)				
		a	b			
2.0	0.000720	0.413251	1.081867	1.0	0.0	0.0
1.988584	0.000697	0.418348	1.073266	0.984	0.10	0.021
1.956736	0.000634	0.431774	1.049056	0.939	1.0	0.089
1.952292	0.000626	0.433560	1.045649	0.933	1.43	0.10
1.939996	0.000603	0.438395	1.036185	0.915	10.0	0.132
1.798911	0.000382	0.483953	0.923071	0.728	--	1.0
1.705399	0.000271	0.505549	0.842400	0.614	--	10.0
			THIRD MODE			
3.0	0.005760	1.036841i	2.432945i	1.0	0.0	0.0
2.989798	0.005668	1.037634i	2.420029i	0.992	0.10	0.0091
2.963754	0.005439	1.039746i	2.386907i	0.972	1.0	0.035
2.951385	0.005333	1.040797i	2.371093i	0.962	10.0	0.048
2.911696	0.005002	1.044397i	2.319959i	0.932	--	0.10
2.737457	0.003720	1.065871i	2.086593i	0.804	--	1.0
2.680194	0.003356	1.075971i	2.005585i	0.763	--	10.0

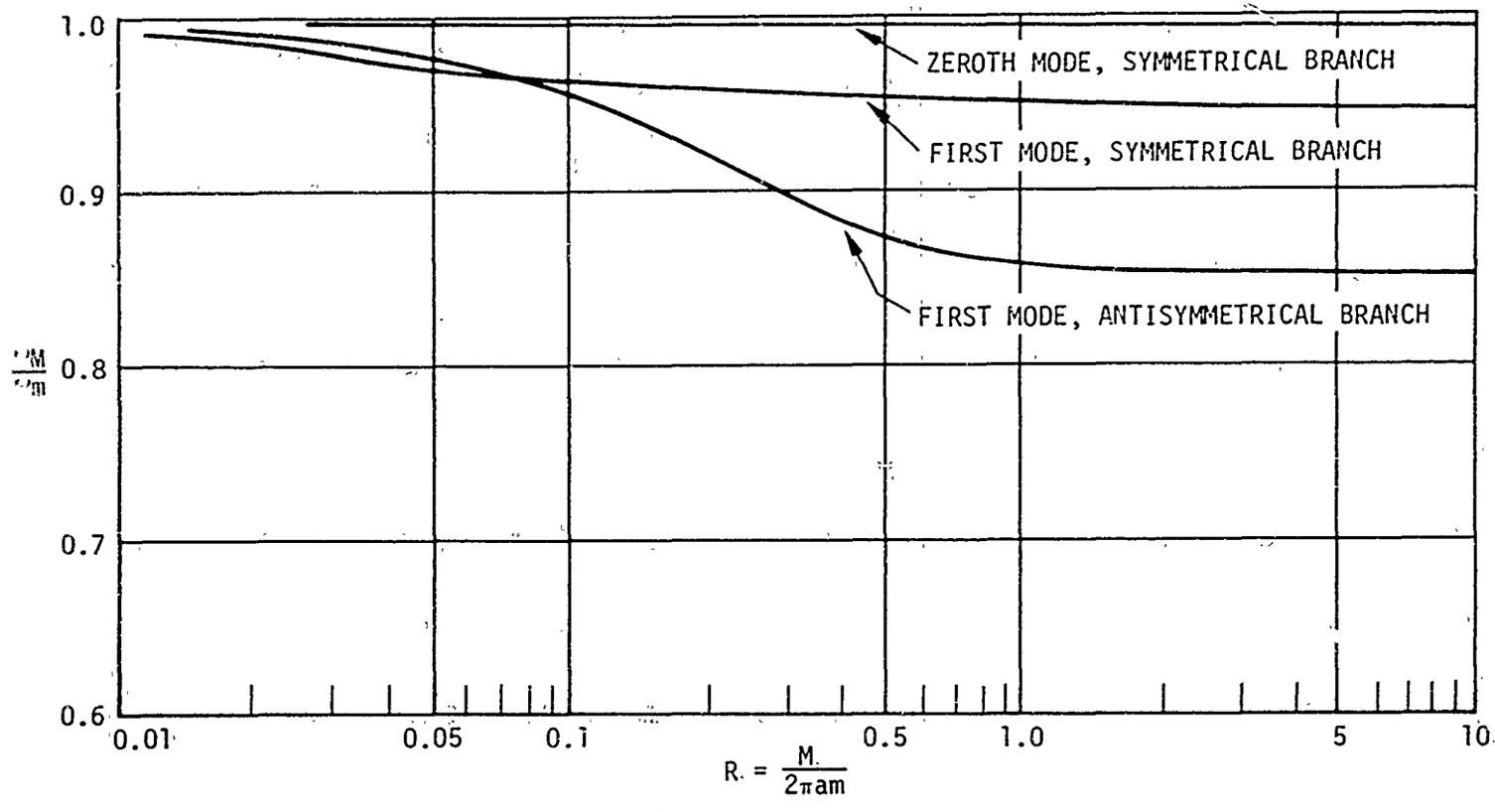

Figure 3 - Variation of Frequency with Mass, Zeroth and First Modes, Extensional Class, Z = 0.0001

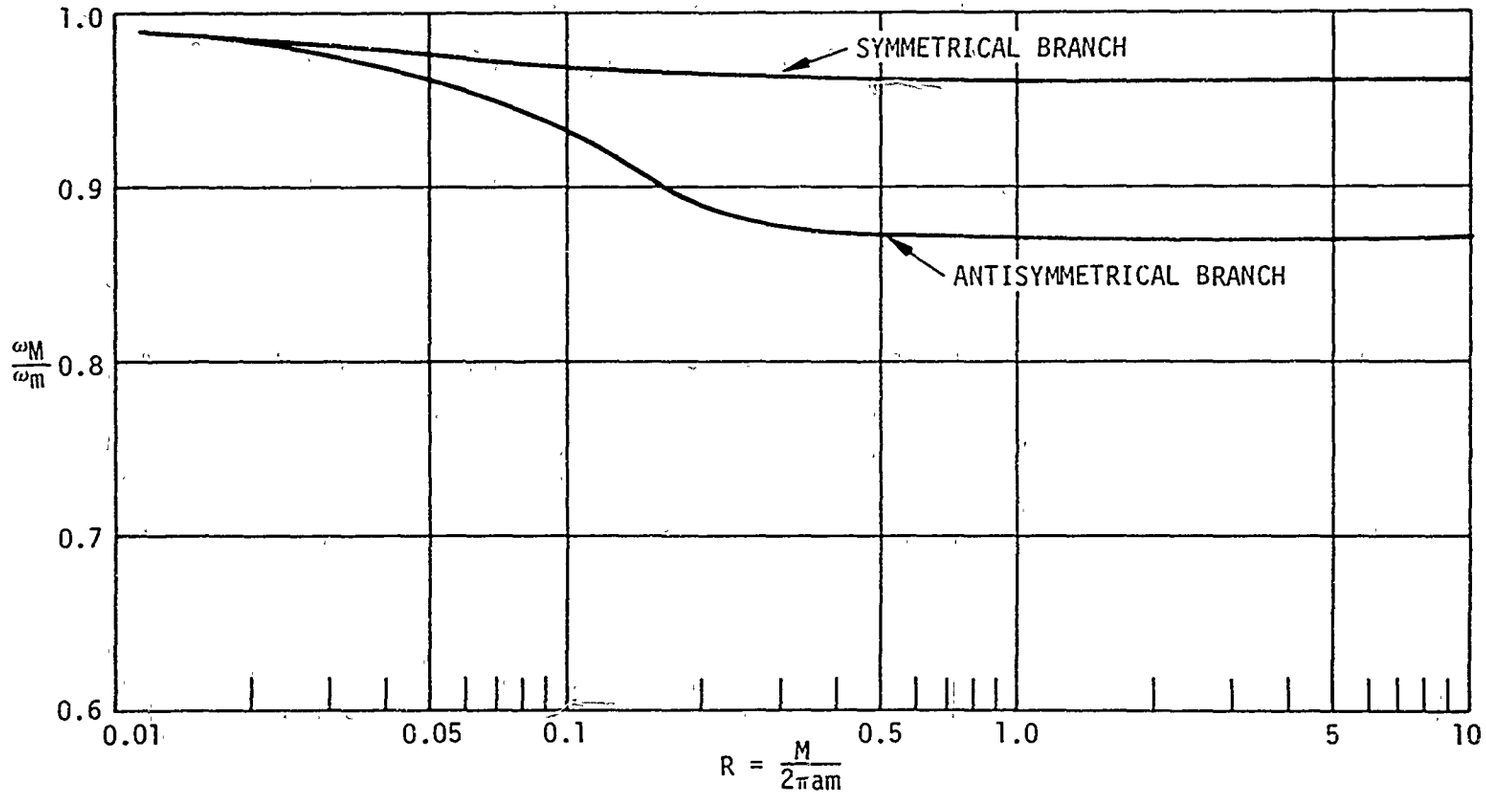

Figure 4 - Variation of Frequency with Mass, Second Mode, Extensional Class, Z = 0.0001

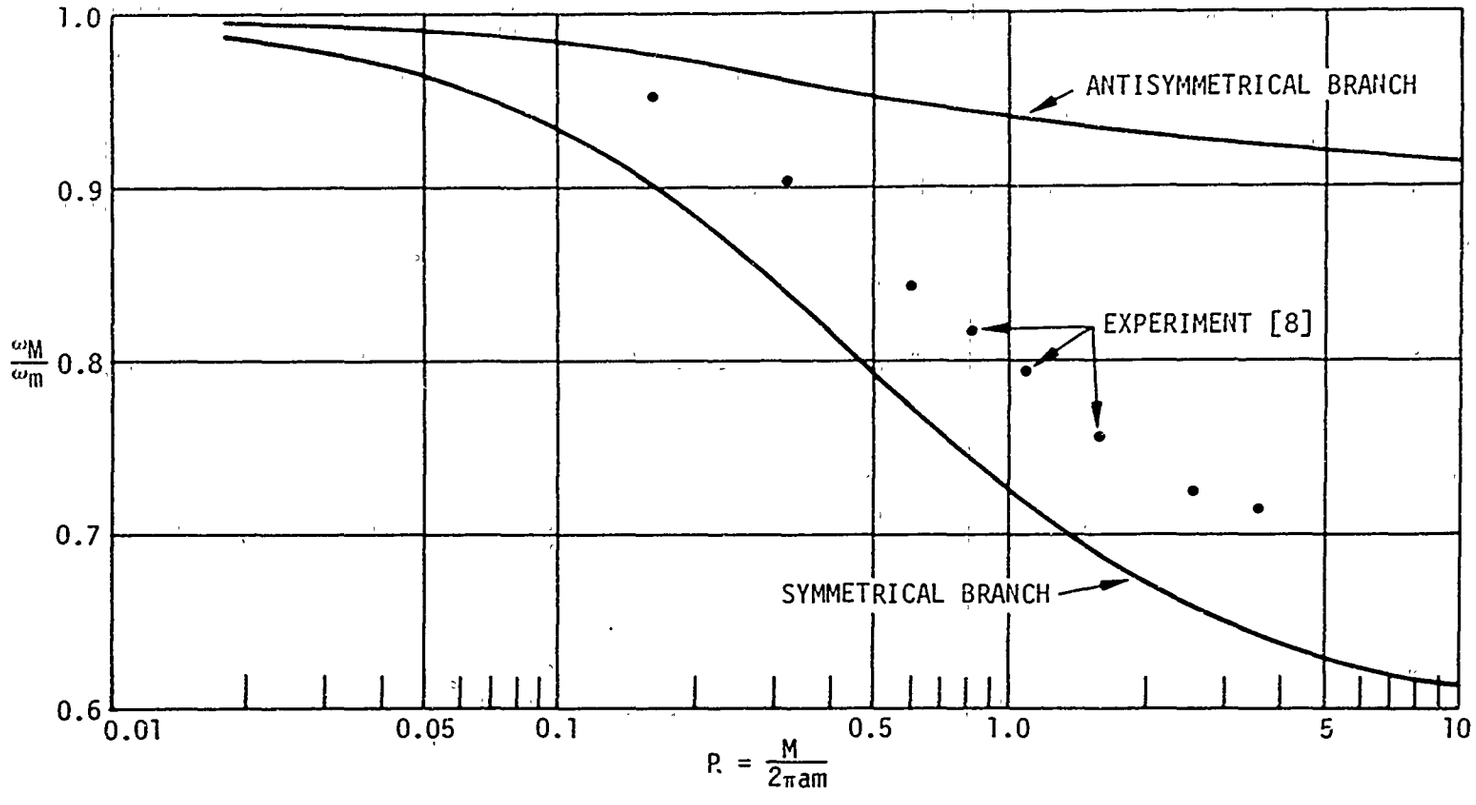

Figure 5 - Variation of Frequency with Mass, Second Mode, Flexural Class, Z = 0.0001

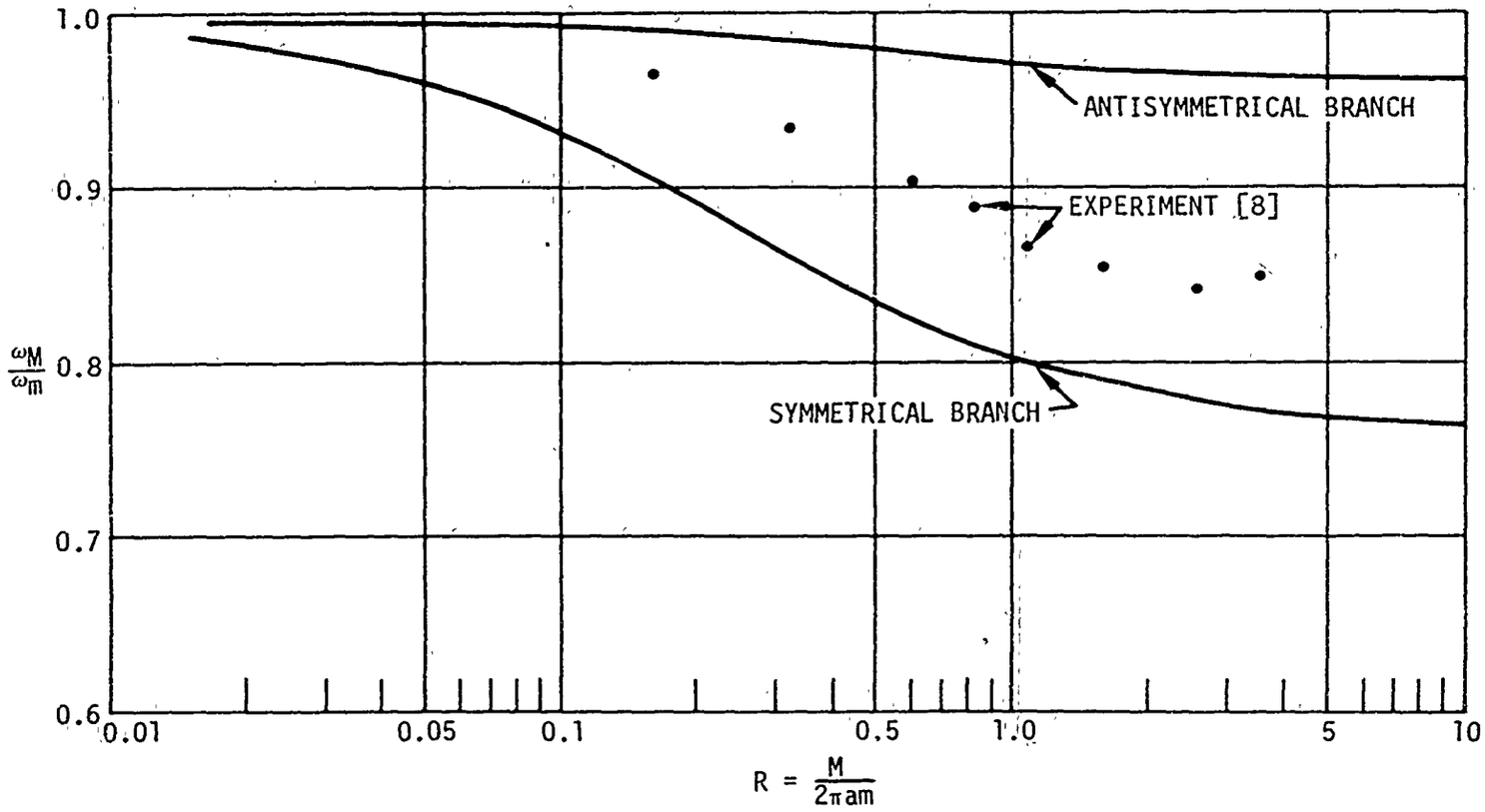

Figure 6 - Variation of Frequency with Mass, Third Mode, Flexural Class, Z = 0.0001

As noted on the figures, the stiffness parameter Z was taken to be 10^{-6}. This particular value of Z represents a ring of unit width, 12 inches in diameter, with a thickness of 0.21 inches. Calculations using other values of Z ranging from 10^{-2} to 10^{-6} showed less than 10% difference with those represented by the figures, with the largest differences occurring in the extensional class modes and virtually no difference in the flexural class particularly for smaller Z values.

3. Influence of Mass on Mode Shapes

Equations (49) through (52) were used to determine the normalized mode shapes for desired values of the mass ratio, R. The parameters, n_k and C, for particular values of R were found by iteration on the process described previously in 1.a. and 1.b.

The normalized displacement function W is shown in Figures 7 and 8 for θ between 0 and 180 degrees.

G. Comparison with Experiment

Lee, et al, [8] conducted an experimental study to determine the effects of added mass on the vibrations of ring structures. By resonance testing, they found flexural symmetric natural frequencies and mode shapes for several values of the mass ratio, R. Their frequency results are shown on Figures 5 and 6 for comparison with present theory. The experimental results show the same general trend as theory for increasing P, but the experimental frequency ratio is, on the average, about 10% higher than theory. For a variety of reasons, precise agreement between theory and experiment generally cannot be expected, especially for vibratory and transient phenomena. In this case the principal cause of disagreement can be attributed to the fact that in

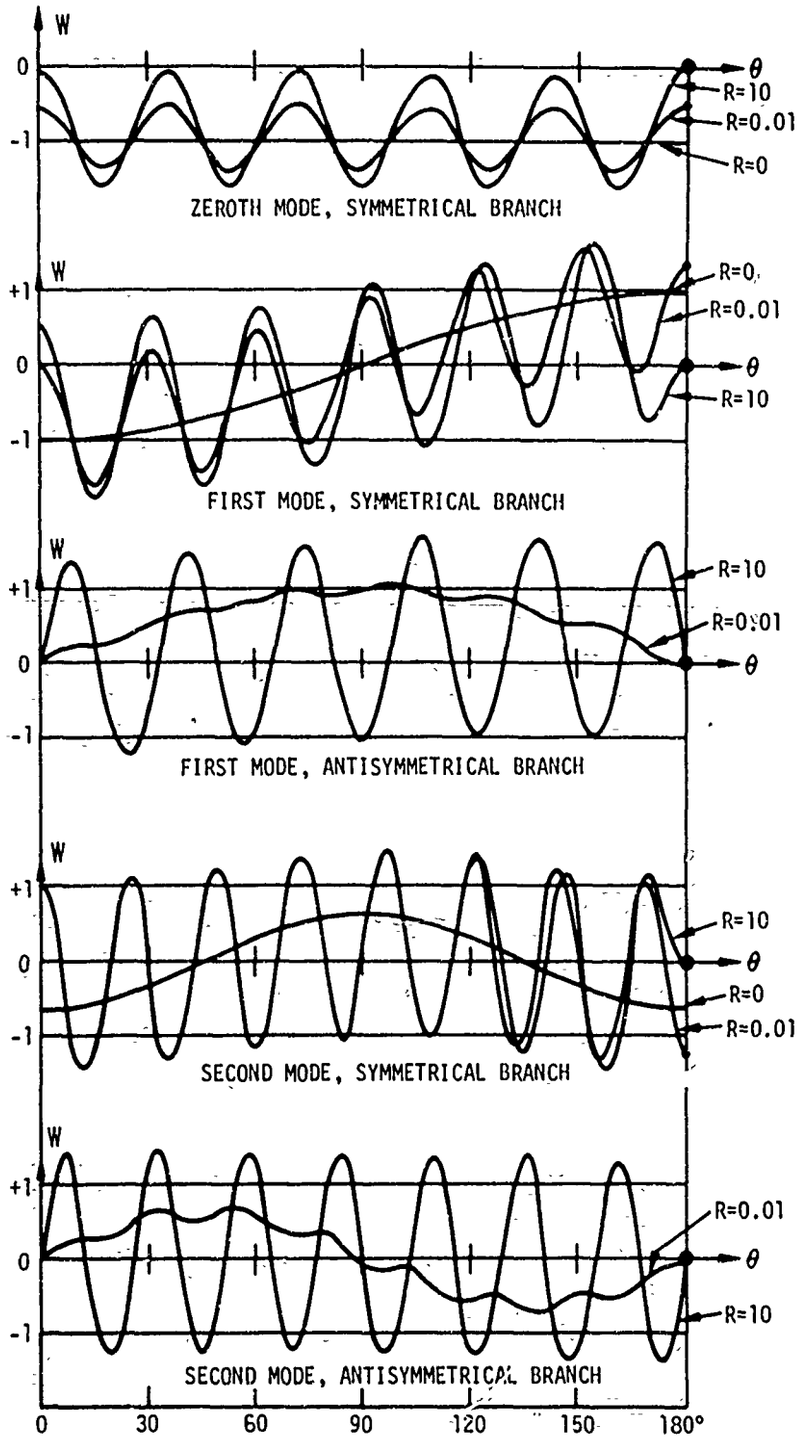

Figure 7 - Normalized Mode Shapes, Extensional Class, Z = 0.0001

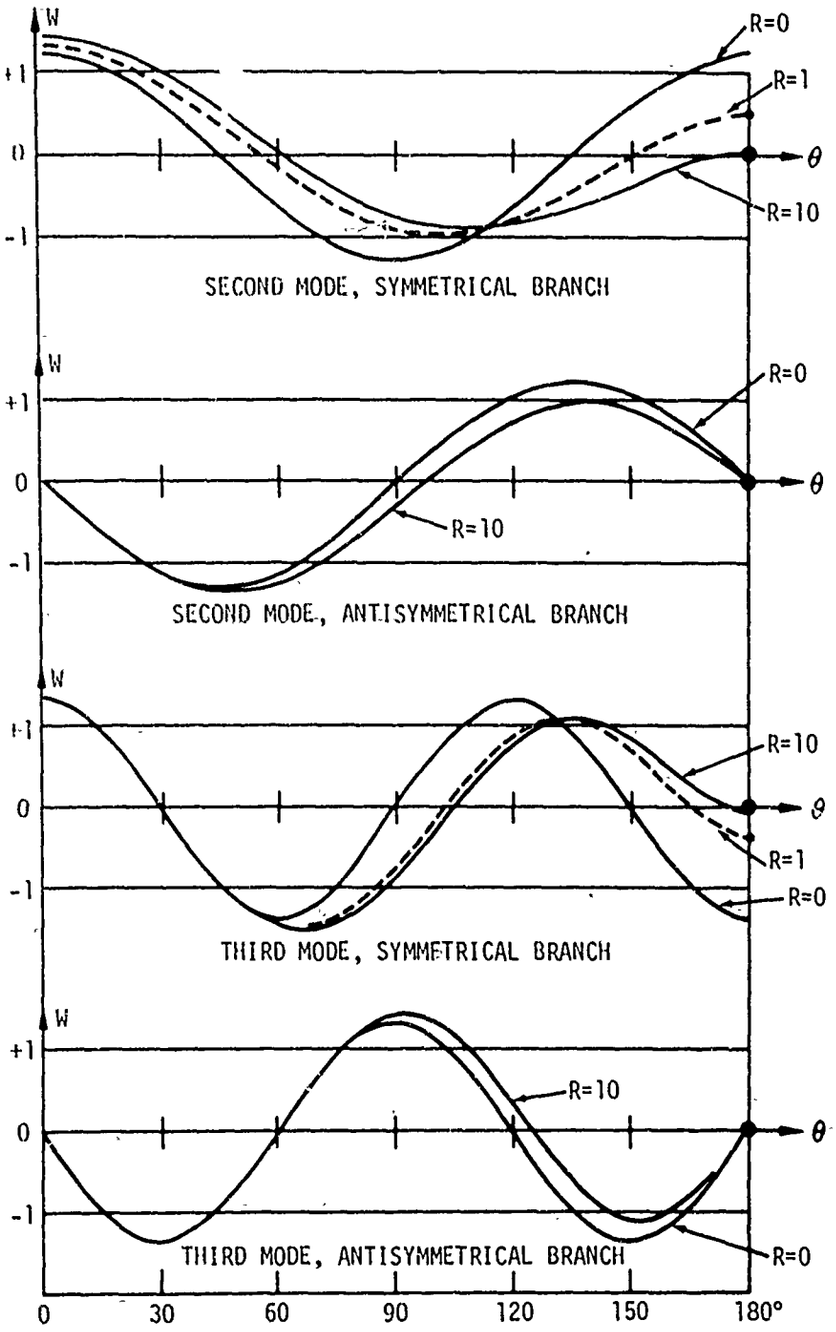

Figure 8 - Normalized Mode Shapes, Flexural Class, Z = 0.0001

the conduct of the experiments the ring was driven eccentrically with respect to the attached mass, thus permitting some participation of the antisymmetric branches. As shown by present theory, this would account for somewhat higher frequency ratios than those that would result from pure symmetric excitation. Experimental mode shapes are shown in Figures 9 and 10 and show the same general trend of reduced amplitude at the mass for increasing R as the theory.

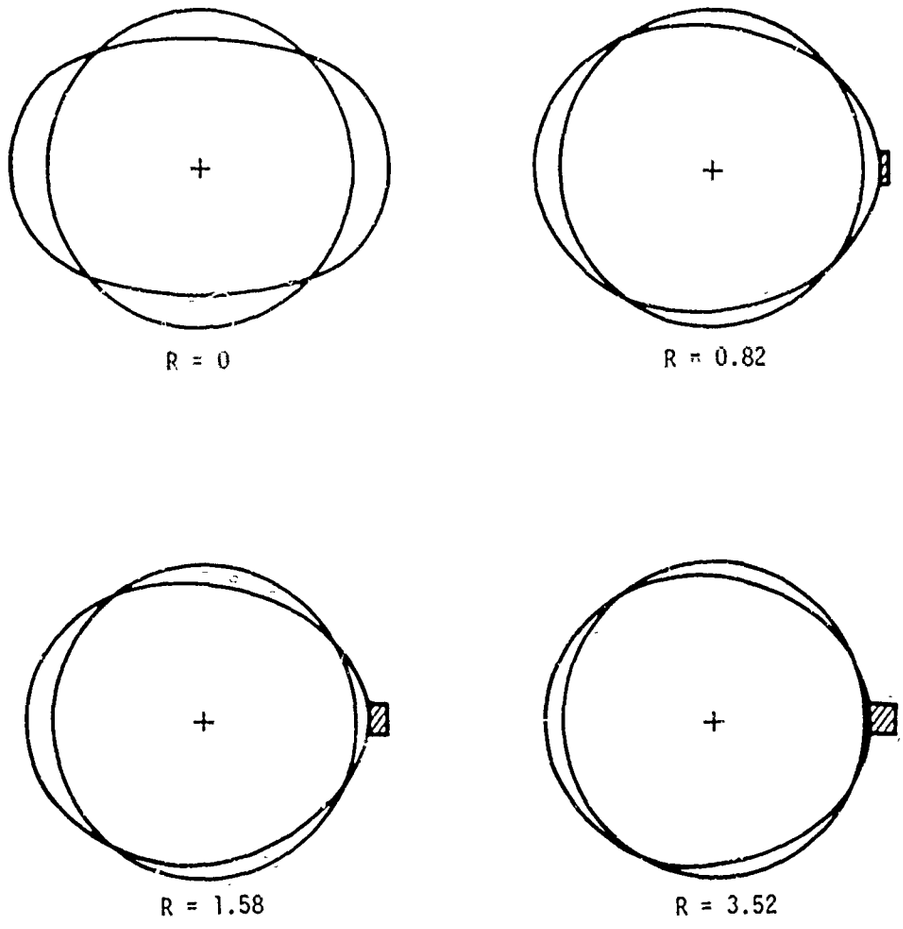

Figure 9 - Experimental [8] Mode Shapes, Second Mode, Flexural Class, Symmetrical Branch, $Z = 2.6 \times 10^{-6}$

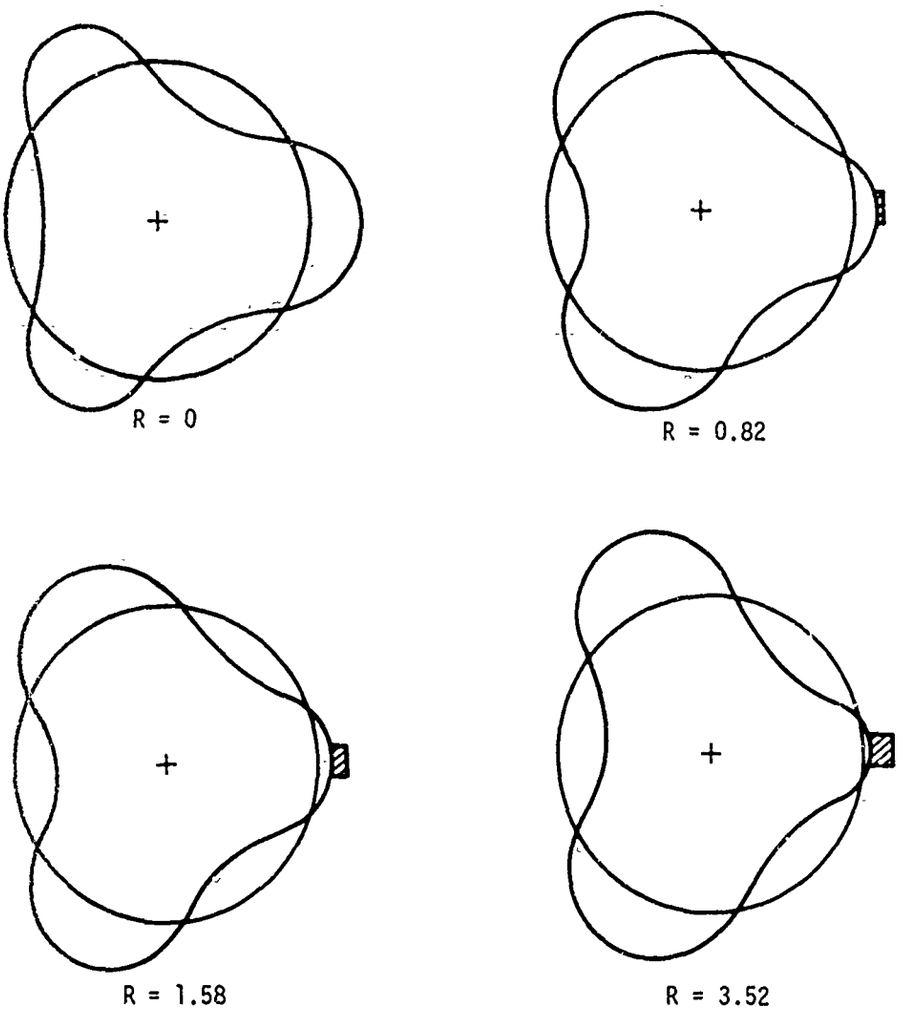

Figure 10 - Experimental [8] Mode Shapes, Third Mode, Flexural Class, Symmetrical Branch, $Z = 2.6 \times 10^{-6}$

II. Discussion

The influence of the added mass on the natural vibrations will be discussed in terms of the solution without added mass.

1. Influence of Mass on Frequencies

An obvious feature here is the difference in frequency between the symmetrical and antisymmetrical branches of a normal mode, as shown in Figures 3 through 6. This holds for both classes of vibration, extensional and flexural. For no added mass, R = 0, both branches of a particular class have the same frequency, but as the added mass increases, the difference in frequency also increases. Note that the zeroth, or breathing, mode has only the symmetrical branch. This is an expected result since for the case of zero added mass, only the symmetrical branch exists, as shown by equations (53) through (56).

For the extensional class modes, as the mass ratio increases, the reduction in frequency is greater in the antisymmetrical branch than in the symmetrical branch. The reverse is true for the flexural class.

With the exception of the zeroth mode, it is noted that for either class, the reduction in frequency is less for both branches for the higher modes than for the lower. The zeroth mode shows very little reduction in frequency regardless of the amount of added mass.

2. Influence of Mass on Mode Shapes

Figures 7 and 8 indicate that the displacement of the added mass decreases as the mass ratio increases. A large added mass tends to become a node. In the flexural class, the mass has appreciably less influence on the antisymmetrical shapes than on the symmetrical, as

shown by Figure 8. The effect of added mass on the extensional class mode shapes is striking. Figure 7 shows the presence of coupling with higher flexural class modes. Even for a very small value of the mass ratio (R = 0.01) this coupling is quite severe, particularly for the symmetrical branches. Observe also that even with this coupling the true character of the extensional shapes is maintained since the flexure is superimposed on the primary extension. This behavior is especially noticeable in the zeroth mode shape shown in Figure 7.

For the uniform cylinder without added mass, it is interesting to note from equations (54) and (56) that the only distinction in shape between the symmetrical and anti-symmetrical branches of a particular mode is that the axis of symmetry of the anti-symmetrical branch shape is rotated $\frac{\pi}{2n}$ radians from the axis of symmetry of the symmetrical branch shape. As shown in Tables 1 and 2, for R = 0, both branches of the same class of vibration have the same natural frequency. Such degeneracy does not exist when the added mass is present. Not only are the anti-symmetrical branch shapes completely without symmetry and different from those of the symmetrical branch, but the frequencies associated with each branch are different as well.

The zeroth and first flexural class modes are non-oscillatory, rigid body modes. They will be treated in the next Chapter.

IV. IMPULSE RESPONSE

The general impulse response solution will be obtained by modal analysis for arbitrary spatial variation of the initial conditions. This general solution will then be specialized to a particular form of the initial conditions for comparison with experimental results. The impulse response of a uniform cylinder (R = 0) will be obtained as a degenerate case of the general impulse response solution.

A. General Solution

As was shown in Chapter III, for each mode of vibration (zeroth, first, etc.), four solutions are possible, symmetric and antisymmetric branches for each of the two classes, flexural and extensional. Since each of the four is a solution and since the problem is linear, then a linear combination of the four solutions is also a solution. Therefore, the displacement components for the i^{th} mode can be written as

$$v_i = v_{eai} + v_{esi} + v_{fai} + v_{fsi} \tag{90}$$

and

$$w_i = w_{eai} + w_{esi} + w_{fai} + w_{fsi} \tag{91}$$

It is convenient to express the spatial and temporal variables of each of the components of equations (90) and (91) as follows

$$v_{eai} = V_{eai}(\bar{c}_i \sin \omega_{eai} t + \bar{d}_i \cos \omega_{eai} t) \tag{92}$$

$$v_{esi} = V_{esi}(c_i \sin \omega_{esi} t + d_i \cos \omega_{esi} t) \tag{93}$$

$$v_{fai} = V_{fai}(\bar{a}_i \sin \omega_{fai} t + \bar{b}_i \cos \omega_{fai} t) \tag{94}$$

$$v_{fsi} = V_{fsi}(a_i \sin \omega_{fsi} t + b_i \cos \omega_{fsi} t) \tag{95}$$

$$w_{eai} = W_{eai} (\bar{c}_i \sin \omega_{eai} t + \bar{d}_i \cos \omega_{eai} t) \tag{96}$$

$$w_{esi} = W_{esi} (c_i \sin \omega_{esi} t + d_i \cos \omega_{esi} t) \tag{97}$$

$$w_{fai} = W_{fai} (\bar{a}_i \sin \omega_{fai} t + \bar{b}_i \cos \omega_{fai} t) \tag{98}$$

$$w_{fsi} = W_{fsi} (a_i \sin \omega_{fsi} t + b_i \cos \omega_{fsi} t) \tag{99}$$

where V_{eai}, W_{eai}, etc., are the mode shapes obtained previously, and a_i, $\bar{a}_i$, b_i, etc., are constants to be obtained from the initial conditions. Summing all the modes gives the complete solution which is

$$v = \sum_{i=0}^{\infty} v_i \tag{100}$$

and

$$w = \sum_{i=0}^{\infty} w_i \tag{101}$$

For given initial conditions on the displacement and velocity, the constants a_i, $\bar{a}_i$, b_i, etc., can be obtained through the orthogonality relation. Let the initial conditions be stated as

$$\begin{aligned} v(\theta,0) &= \bar{v} \\ w(\theta,0) &= \bar{w} \\ \dot{v}(\theta,0) &= \dot{\bar{v}} \\ \dot{w}(\theta,0) &= \dot{\bar{w}} \end{aligned} \tag{102}$$

Then, from equations (100) and (101), with (102) we have

$$\sum_{i=0}^{\infty} v_i(\theta,0) = \bar{v} \tag{103}$$

$$\sum_{i=0}^{\infty} w_i(\theta,0) = \bar{w} \tag{104}$$

$$\sum_{i=0}^{\infty} \dot{v}_i(\theta,0) = \dot{\bar{v}} \tag{105}$$

and

$$\sum_{i=0}^{\infty} \dot{w}_i(\theta,0) = \dot{\bar{w}} \tag{106}$$

The object now is to manipulate equations (103) through (106) to forms such that the orthogonality condition, equation (57), can be employed. To obtain a_i and b_i, for example, multiply (103) and (105) by $V_{fsj}\mathrm{mad}\theta$, and (104) and (106) by $W_{fsj}\mathrm{mad}\theta$ and integrate, which gives

$$\sum_{i=0}^{\infty} \int_{-\pi}^{\pi} v_i(\theta,0)\, V_{fsj}\mathrm{mad}\theta = \int_{-\pi}^{\pi} \bar{v} V_{fsj}\mathrm{mad}\theta \tag{107}$$

$$\sum_{i=0}^{\infty} \int_{-\pi}^{\pi} v_i(\theta,0)\, V_{fsj}\mathrm{mad}\theta = \int_{-\pi}^{\pi} \dot{\bar{v}} V_{fsj}\mathrm{mad}\theta \tag{108}$$

$$\sum_{i=0}^{\infty} \int_{-\pi}^{\pi} w_i(\theta,0)\, W_{fsj}\mathrm{mad}\theta = \int_{-\pi}^{\pi} \bar{w} W_{fsj}\mathrm{mad}\theta \tag{109}$$

$$\sum_{i=0}^{\infty} \int_{-\pi}^{\pi} \dot{w}_i(\theta,0)\, W_{fsj}\mathrm{mad}\theta = \int_{-\pi}^{\pi} \dot{\bar{w}} W_{fsj}\mathrm{mad}\theta \tag{110}$$

For $\theta = \pi$, the location of the added mass, equations (103) through (106) become

$$\sum_{i=0}^{\infty} v_i(\pi,0) = \bar{v}(\pi) \tag{111}$$

$$\sum_{i=0}^{\infty} w_i(\pi,0) = \bar{w}(\pi) \tag{112}$$

$$\sum_{i=0}^{\infty} \dot{v}_i(\pi,0) = \dot{\bar{v}}(\pi) \tag{113}$$

$$\sum_{i=0}^{\infty} \dot{w}_i(\pi,0) = \dot{\bar{w}}(\pi) \tag{114}$$

Multiplying equations (111) and (113) by $MV_{fsj}^{(\pi)}$ and (112) and (114) by $MW_{fsj}^{(\pi)}$ gives

$$\sum_{i=0}^{\infty} Mv_i(\pi,0)\, V_{fsj}^{(\pi)} = M\bar{v}(\pi)\, V_{fsj}^{(\pi)} \tag{115}$$

$$\sum_{i=0}^{\infty} M\dot{v}_i(\pi,0)\, V_{fsj}^{(\pi)} = M\dot{\bar{v}}(\pi)\, V_{fsj}^{(\pi)} \tag{116}$$

$$\sum_{i=0}^{\infty} Mw_i(\pi,0)\, W_{fsj}^{(\pi)} = M\bar{w}(\pi)\, W_{fsj}^{(\pi)} \tag{117}$$

$$\sum_{i=0}^{\infty} M\dot{w}_i(\pi,0)\, W_{fsj}^{(\pi)} = M\dot{\bar{w}}(\pi)\, W_{fsj}^{(\pi)} \tag{118}$$

Adding equations (107), (109), (115) and (117) results in

$$\sum_{i=0}^{\infty} \left\{ \int_{-\pi}^{\pi} \left[v_i(\theta,0)\, V_{fsj} + w_i(\theta,0)\, W_{fsj} \right] mad\theta + M \left[v_i(0)\, V_{fsj} + w_i(0)\, W_{fsj} \right]_{\pi} \right\}$$

$$= \int_{-\pi}^{\pi} \left[\bar{v} V_{fsj} + \bar{w} W_{fsj} \right] mad\theta + M \left[\bar{v} V_{fsj} + \bar{w} W_{fsj} \right]_{\pi} \tag{119}$$

Using equations (90) through (99), and the orthogonality condition, equation (57), it follows that all the terms on the left hand side of equation (119) are zero except those in which i = j and are of the flexural class, symmetrical branch. This latter condition is an important point since even for the same mode number of vibration (i = j), there are four solution states, each in general having a different natural frequency and normal mode shape. Thus equation (119) yields the constants b_i,

$$b_i = \frac{\int_{-\pi}^{\pi} \left[\bar{v}V_{fsi} + \bar{w}W_{fsi}\right] m a d\theta + M\left[\bar{v}V_{fsi} + \bar{w}W_{fsi}\right]_{\pi}}{\int_{-\pi}^{\pi} \left[V_{fsi}^2 + W_{fsi}^2\right] m a d\theta + M\left[V_{fsi}^2 + W_{fsi}^2\right]_{\pi}} \tag{120}$$

Using normalized functions as given by equation (58), equation (120) may be written as

$$b_i = \frac{1}{2\pi}\int_{-\pi}^{\pi} \left[\bar{v}V_{fsi} + \bar{w}W_{fsi}\right] d\theta + R\left[\bar{v}V_{fsi} + \bar{w}\dot{W}_{fsi}\right]_{\pi} \tag{121}$$

Adding equations (108), (110), (116) and (118), and following the same procedure, the constants a_i are found to be

$$a_i = \frac{\frac{1}{2\pi}\int_{-\pi}^{\pi} \left[\dot{\bar{v}}V_{fsi} + \dot{\bar{w}}W_{fsi}\right] d\theta + R\left[\dot{\bar{v}}V_{fsi} + \dot{\bar{w}}W_{fsi}\right]_{\pi}}{\omega_{fsi}} \tag{122}$$

Through a procedure similar to the above, the other constants in equations (92) through (98) are found to be

$$c_i = \frac{\frac{1}{2\pi}\int_{-\pi}^{\pi} \left[\dot{\bar{v}}V_{esi} + \dot{\bar{w}}W_{esi}\right] d\theta + R\left[\dot{\bar{v}}V_{esi} + \dot{\bar{w}}W_{esi}\right]_{\pi}}{\omega_{esi}} \tag{123}$$

$$d_i = \frac{1}{2\pi}\int_{-\pi}^{\pi}\left[\bar{v}V_{esi} + \bar{w}W_{esi}\right] d\theta + R\left[\bar{v}V_{esi} + \bar{w}W_{esi}\right]_{\pi} \tag{124}$$

$$\bar{a}_i = \frac{\frac{1}{2\pi}\int_{-\pi}^{\pi}\left[\dot{\bar{v}}V_{fai} + \dot{\bar{w}}W_{fai}\right] d\theta + R\left[\dot{\bar{v}}V_{fai} + \dot{\bar{w}}W_{fai}\right]_{\pi}}{\omega_{fai}} \tag{125}$$

$$\bar{b}_i = \frac{1}{2\pi}\int_{-\pi}^{\pi}\left[\bar{v}V_{fai} + \bar{w}W_{fai}\right] d\theta + R\left[\bar{v}V_{fai} + \bar{w}W_{fai}\right]_{\pi} \tag{126}$$

$$\bar{c}_i = \frac{\frac{1}{2\pi}\int_{-\pi}^{\pi}\left[\dot{\bar{v}}V_{eai} + \dot{\bar{w}}W_{eai}\right] d\theta + R\left[\dot{\bar{v}}V_{eai} + \dot{\bar{w}}W_{eai}\right]_{\pi}}{\omega_{eai}} \tag{127}$$

$$\bar{d}_i = \frac{1}{2\pi}\int_{-\pi}^{\pi}\left[\bar{v}V_{eai} + \bar{w}W_{eai}\right] d\theta + R\left[\bar{v}V_{eai} + \bar{w}W_{eai}\right]_{\pi} \tag{128}$$

Equations (123), (124), (127), and (128) associated with the extensional class are valid for any mode number, i, equal to or greater than zero. Equations (121), (122), (125) and (126) associated with the flexural class are valid only for mode numbers equal to or greater than two. As shown previously in Chapter III, harmonic solutions are not possible for the zeroth and first modes of the flexural class. Therefore these must be treated separately. Previous analytical studies [10,19] of the flexural response of uniform rings have shown that the zeroth and first flexural class modes are associated with rigid body motions. The solution for the zeroth mode can be taken as follows

$$v_{f0} = f_0 + h_0 t \text{ and } w_{f0} = g_0 + k_0 t \tag{129}$$

Substituting (129) into the governing equations (6) and (7), it is found that $g_o = k_o = 0$ and f_o and h_o are arbitrary, which represents a rigid body rotation. For the first mode, the solution is taken as

$$v_{11} = (f_1 + h_1 t)\sin\theta \text{ and } w_{11} = (g_1 + k_1 t)\cos\theta \tag{130}$$

Upon substituting (130) into equations (6) and (7), it is found that the governing equations are satisfied by equations (130) if $f_1 = g_1$ and $h_1 = k_1$. Note that this solution represents a rigid body translation. The non-harmonic or zero frequency solutions for the zeroth and first flexural class modes given by equations (129) and (130) also satisfy the equilibrium and continuity conditions, equations (15) through (20), thus are valid solutions to the given problem. The orthogonality relation, equation (57), also is applicable for these solutions.

Proceeding in the same manner as before, the constants f_o, h_o, f_1 and h_1 are found to be

$$f_0 = \frac{\frac{1}{2\pi}\int_{-\pi}^{\pi} \bar{v}\,d\theta + R\bar{v}(\pi)}{1+R} \tag{131}$$

$$h_0 = \frac{\frac{1}{2\pi}\int_{-\pi}^{\pi} \dot{\bar{v}}\,d\theta + R\dot{\bar{v}}(\pi)}{1+R} \tag{132}$$

$$f_1 = \frac{\frac{1}{2\pi}\int_{-\pi}^{\pi} \left[\bar{v}\sin\theta + \bar{w}\cos\theta\right] d\theta - R\bar{w}(\pi)}{1+R} \tag{133}$$

$$h_1 = \frac{\frac{1}{2\pi}\int_{-\pi}^{\pi} \left[\dot{\bar{v}}\sin\theta + \dot{\bar{w}}\cos\theta\right] d\theta - R\dot{\bar{w}}(\pi)}{1+R} \tag{134}$$

Thus, with all the constants determined from equations (121) through (128) and (131) and (134), the complete general solution is

$$v = f_0 + h_0 t + (f_1 + h_1 t)\sin\theta + \sum_{i=2}^{\infty} v_{fi} + \sum_{i=0}^{\infty} v_{ei} \tag{135}$$

and

$$w = (f_1 + h_1 t)\cos\theta + \sum_{i=2}^{\infty} w_{fi} + \sum_{i=0}^{\infty} w_{ei} \tag{136}$$

where $v_{fi} = v_{fai} + v_{fsi}$

$v_{ei} = v_{eai} + v_{esi}$

$w_{fi} = w_{fai} + w_{fsi}$

and $w_{ei} = w_{eai} + w_{esi}$

The impulse response solution for a uniform cylinder without added mass has the same form as above and may be derived from the above general solution by setting R = 0 and using the mode shapes given by equations (53) through (56).

B. Solution for Specified Initial Conditions

For later comparison with experimental results, the impulse response solution for a particular set of initial conditions will now be obtained. Let the initial conditions be of the following form:

$$\begin{aligned} &\bar{v} = \dot{\bar{v}} = \bar{w} = 0 \quad , \quad \text{for all } \theta \\ &\dot{\bar{w}} = -\dot{\bar{w}}_0 \cos\theta \quad , \quad \text{for } \pi \geq \theta \geq \frac{\pi}{2} \\ &\qquad\qquad \text{and} \quad \text{for } -\frac{\pi}{2} \geq \theta \geq -\pi \\ &\dot{\bar{w}} = 0 \quad , \quad \text{for } -\frac{\pi}{2} < \theta < \frac{\pi}{2} \end{aligned} \tag{137}$$

where $\bar{w}_0$ is a specified amplitude constant.

With the above initial conditions, the mode constants are determined from equations (121) through (128) and (131) through (134) and are

$$a_0 \quad b_0 \quad a_1 \quad 0$$

$$b_1 \quad \frac{-\bar{w}_0(a_1 + R)}{1 + R}$$

$$\bar{a}_1 \quad b_1 \quad \bar{b}_1 \quad c_1 \quad d_1 \quad \bar{d}_1 \quad 0 \tag{138}$$

$$a_1 \quad \frac{\bar{w}_0 B_{1fsi}}{\omega_{fsi}} \left\{ \frac{RW_{fsi}^{\pi}}{B_{1fsi}} - \frac{1}{\pi} \left[(n_{1fsi}^2 - C_{fsi}) F_{1t} + (n_{2fsi}^2 - C_{fsi}) \frac{B_{2fsi}}{B_{1fsi}} F_{2t} \right. \right.$$

$$\left. \left. + (n_{3fsi}^2 - C_{fsi}) \frac{B_{3fsi}}{B_{1fsi}} F_{3t} \right] \right\}, \quad t > 0 \tag{139}$$

$$c_1 \quad \frac{\bar{w}_0 B_{1esi}}{\omega_{esi}} \left\{ \frac{RW_{esi}^{\pi}}{B_{1esi}} - \frac{1}{\pi} \left[(n_{1esi}^2 - C_{esi}) F_{1t} + (n_{2esi}^2 - C_{esi}) \frac{B_{2esi}}{B_{1esi}} F_{2t} \right. \right.$$

$$\left. \left. + (n_{3esi}^2 - C_{esi}) \frac{B_{3esi}}{B_{1esi}} F_{3t} \right] \right\}, \quad t \geq 0 \tag{140}$$

where

$$F_{ki} = \frac{\sin(1 - n_{kfsi})\pi}{2(1 - n_{kfsi})} + \frac{\sin(1 + n_{kfsi})\pi}{2(1 + n_{kfsi})} - \frac{\sin(1 - n_{kfsi})\frac{\pi}{2}}{2(1 - n_{kfsi})} - \frac{\sin(1 + n_{kfsi})\frac{\pi}{2}}{2(1 + n_{kfsi})}$$

$$E_{ki} = \frac{\sin(1 - n_{kesi})\pi}{2(1 - n_{kesi})} + \frac{\sin(1 + n_{kesi})\pi}{2(1 + n_{kesi})} - \frac{\sin(1 - n_{kesi})\frac{\pi}{2}}{2(1 - n_{kesi})} - \frac{\sin(1 + n_{kesi})\frac{\pi}{2}}{2(1 + n_{kesi})}$$

$k = 1, 2, 3$

W_{fsi} and W_{esi} are obtained from equation (52). The constants B_{1fsi} and B_{1esi} are found from equation (62), and $\frac{B_{2fsi}}{B_{1fsi}}$, $\frac{B_{2esi}}{B_{1esi}}$, $\frac{B_{3fsi}}{B_{1fsi}}$, and $\frac{B_{3esi}}{B_{1esi}}$ are given by equations (47) and (48). The natural frequency, ω_i, is found from equation (13), and is

$$\omega_i = \frac{1}{a}\sqrt{\frac{C_i \bar{E} A}{m}}$$

The complete solution is

$$v = h_1 t \sin\theta + \sum_{i=2}^{\infty} a_i V_{fsi} \sin\omega_{fsi} t + \sum_{i=0}^{\infty} c_i V_{esi} \sin\omega_{esi} t \qquad (141)$$

$$r = h_1 t \cos\theta + \sum_{i=2}^{\infty} a_i W_{fsi} \sin\omega_{fsi} t + \sum_{i=0}^{\infty} c_i W_{esi} \sin\omega_{esi} t \qquad (142)$$

In the above treatment, it is emphasized that the mode shapes V_i and W_i are normalized in accordance with equation (59).

For the case of a uniform cylinder, R = 0, the form of solution given by equations (141) and (142) remains the same; however, the expressions for the constants h_1, a_i and c_i are simplified. Equation

(138) becomes

$$b_1 = -\frac{\dot{\bar{w}}_0}{4} \tag{143}$$

equation (139) becomes

$$a_n = -\frac{\dot{\bar{w}}_0 B_{1fsn}}{\pi\omega_{fsn}}(n^2 - C_{fsn}) F_{1n}, \quad n \geq 2 \tag{144}$$

and equation (140) becomes

$$c_n = -\frac{\dot{\bar{w}}_0 B_{1esn}}{\pi\omega_{esn}}(n^2 - C_{esn}) E_{1n}, \quad n \geq 0 \tag{145}$$

Note that the mode number now is the same as the integer n.

Other response parameters, such as velocity and stress, can be obtained by appropriate temporal and spatial differentiation of the displacements given by equations (141) and (142).

C. Comparison with Experimental Results

Several specific numerical solutions will now be obtained for comparison with available experimental results.

1. Cylinder with Added Mass

The cylinder is impulsively loaded by a shockwave from a nearby underwater explosion. The pertinent parameters for this problem are:

$E = 29 \times 10^6$ (psi)

$\nu = 0.3$

$a = 8.65$ (ft)

$m = 0.0502 \left(\frac{lb - sec^2}{in^2}\right)$

$Z = 0.00194$

$R = 0.18$

It is desired to compare with Navy experimental radial velocity measurements recorded at the location of the added mass, $\theta = \pi$. Differentiating equation (142) with respect to time, we obtain the following expression for the non-dimensional radial velocity at $\theta = \pi$:

$$\frac{\dot{w}(\pi,t)}{\dot{\bar{w}}_0} = \frac{\frac{1}{2} + R}{1 + R} + \sum_{i=2}^{\infty} a_i' \cos \omega_{fsi} t + \sum_{i=0}^{\infty} c_i' \cos \omega_{esi} t \qquad (146)$$

where

$$a_i' = \frac{W_{fsi}^{(\pi)} \omega_{fsi}}{\dot{\bar{w}}_0} a_i$$

and

$$c_i' = \frac{W_{esi}^{(\pi)} \omega_{esi}}{\dot{\bar{w}}_0} c_i$$

The amplitude constants a_i' and c_i' are listed in Table 3 through eight modes ($i = 8$). A measure of convergence is indicated by the values shown in Table 3 since both a_i' and c_i' become very small for the higher modes. In fact, these amplitude constants are insignificant for $i > 4$. Figure 11 shows the solution, equation (146), summed through eight modes. Shown also in Figure 11 is the experimental velocity history from reference [20]. The high frequency oscillations on the experimental histories are due primarily to the response of the velocity meter elements. The fundamental natural frequencies of the elements were measured and found to correspond with the superimposed high-frequency oscillations of the experimental records. This is discussed further in reference [21], together with other details of the Navy experimental program.

TABLE 3 - VELOCITY MODE AMPLITUDES, $\theta = \pi$, Z = 0.00194

	R = 0		R = 0.18	
i, n	a'_n	c'_n	a'_i	c'_i
0	0	0.3183	0	0.2112
1	0.25	0.25	0.3644	0.0917
2	0.1696	0.0424	0.2534	0.0067
3	0	0	0.0829	-0.0004
4	-0.0398	-0.0026	0.0652	-0.0013
5	0	0	0	-0.0008
6	0.0176	0.0006	-0.0289	-0.0005
7	0	0	-0.0064	0
8	-0.0099	-0.0002	-0.0084	0

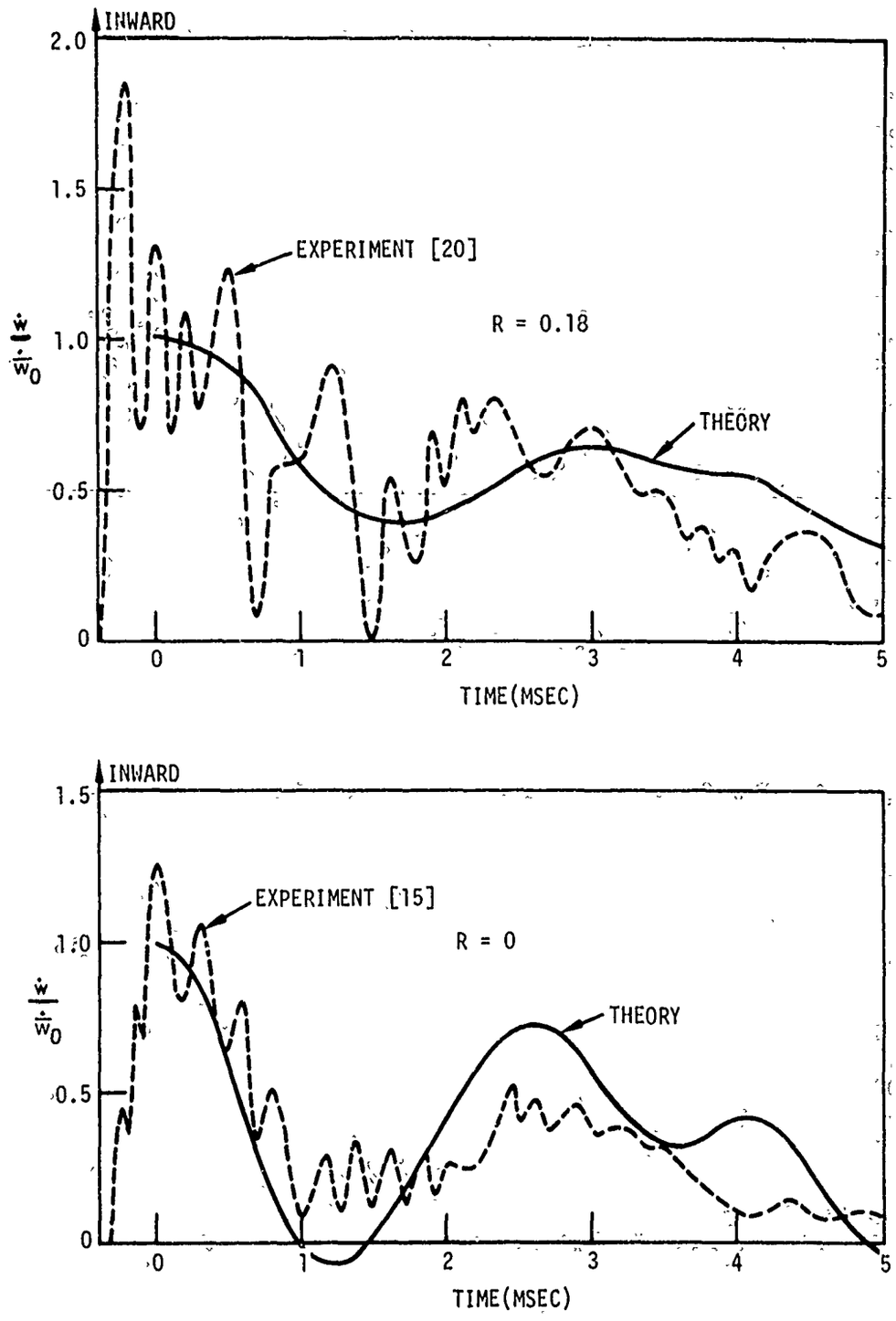

Figure 11 - Theoretical and Experimental Velocity Histories, $\theta = \pi$, $Z = 0.00194$

2. Cylinder without Added Mass

The parameters of the previous problem apply here, except that R = 0. The solution in this case is

$$\frac{\dot{w}(\pi,t)}{\dot{w}_0} = \frac{1}{4} + \sum_{n=2}^{\infty} a'_n \cos \omega_{fsn} t + \sum_{n=0}^{\infty} c'_n \cos \omega_{esn} t \qquad (147)$$

where

$$a'_n = \frac{2(-1)^{\frac{n}{2}} (n^2 - C_{fsn})^2}{\pi(1 - n^2)\left[(n^2 - C_{fsn})^2 + n^2\right]}, \quad n = 2, 4, 6, \cdots$$

$$a'_n = 0, \quad n = 3, 5, 7, \cdots$$

$$c'_0 = \frac{1}{\pi}$$

$$c'_1 = \frac{1}{4}$$

$$c'_n = \frac{2(-1)^{\frac{n}{2}} (n^2 - C_{esn})^2}{\pi(1 - n^2)\left[(n^2 - C_{esn})^2 + n^2\right]}, \quad n = 2, 4, 6, \cdots$$

$$c'_n = 0, \quad n = 3, 5, 7, \cdots$$

The above amplitude constants are listed in Table 3 for eight modes (n = 8). Both of the above expressions for a'_n and c'_n rapidly become very small for large n as is shown by the values in Table 3. The velocity history computed from equation (147) summed through eight modes is shown in Figure 11, together with the experimental velocity history reported in [15] for the case of R = 0.

Both of the theoretical velocity histories shown in Figure 11 are in reasonable agreement with the primary characteristics of the experimental histories. The influence of the added mass can be seen by comparing the upper and lower histories of Figure 11. For the case of

added mass, the velocity generally is at a higher level and does not oscillate to the degree observed for the case of the uniform cylinder without added mass. This can be attributed to increased amplitude in the rigid body translation mode when the added mass is present and reduced participation of the extensional class oscillatory modes, as shown by the mode amplitude constants given in Table 3.

The theoretical solutions shown in Figure 11 were obtained by summation through the eighth mode (i, n = 8). Solutions were also obtained by summation through the sixth mode and the difference between the sixth and eighth mode solutions were found to be on t' order of one percent.

3. Ring without Added Mass

The theory will now be compared with experimental data [16] obtained from strain gages on the inside surface of a 6061 aluminum, 7 inch outside diameter, 1/8 inch thick, one inch wide ring impulsively loaded by a magnetically-driven flyer plate. The pertinent parameters are:

$$E = 10 \times 10^{6} \text{ (psi)}$$

$$a = 3.4375 \text{ (inches)}$$

$$m = 3.1703 \times 10^{-5} \left(\frac{\text{lb - sec}^2}{\text{in}^2}\right)$$

$$Z = 0.00011$$

$$R = 0$$

Substituting equations (141) and (142), with appropriate spatial differentiations, into equations (22) and (23), the stress resultants are obtained,

$$T = \dot{\bar{w}}_0 \frac{EA}{a}\left\{-\frac{1+Z}{\pi\omega_{es0}}\sin\omega_{es0}t + \frac{\cos\theta\sin\omega_{es1}t}{2\omega_{es1}}\right.$$

$$\left. + \sum_{n=2,4,6,\ldots}^{\infty} \frac{2(-1)^{\frac{n}{2}}\cos n\theta}{\pi(1-n^2)}\left[n^2\Gamma_n + [Z(n^2-1)-1]\,\Gamma_n'\right]\right\} \qquad (148)$$

$$G = \dot{\bar{w}}_0 EAZ\left\{\frac{\sin\omega_{es0}t}{\pi\omega_{es0}} + \sum_{n=2,4,6,\ldots}^{\infty}\frac{2(-1)^{\frac{n}{2}}}{\pi}\cos n\theta\,\Gamma_n'\right\} \qquad (149)$$

where

$$\Gamma_n = \frac{(n^2 - C_{fsn})\sin\omega_{fsn}t}{\omega_{fsn}[(n^2 - C_{fsn})^2 + n^2]} + \frac{(n^2 - C_{esn})\sin\omega_{esn}t}{\omega_{esn}[(n^2 - C_{esn})^2 + n^2]}$$

and

$$\Gamma_n' = \frac{(n^2 - C_{fsn})^2\sin\omega_{fsn}t}{\omega_{fsn}[(n^2 - C_{fsn})^2 + n^2]} + \frac{(n^2 - C_{esn})^2\sin\omega_{esn}t}{\omega_{esn}[(n^2 - C_{esn})^2 + n^2]}$$

To obtain non-dimensional stresses on the inside surface of the ring, the following expressions are employed:

$$\frac{\sigma_T h}{I_0 c} = \frac{T}{\rho\dot{\bar{w}}_0 Ac}$$

$$\frac{\sigma_G h}{I_0 c} = \frac{6G}{\rho h\dot{\bar{w}}_0 Ac}$$

where σ_T is the stress due to thrust

σ_G is the stress due to bending

h is the ring thickness

c is the material sound velocity, $\sqrt{\frac{E}{\rho}}$

I_0 is the maximum impulse amplitude, $I_0 = \rho h\dot{\bar{w}}_0$

Thus, the total stress in non-dimensional form at any position on the inside surface of the ring is given by

$$\frac{\sigma h}{I_0 c} = \frac{\sigma_T h}{I_0 c} + \frac{\sigma_G h}{I_0 c} \tag{150}$$

It is also desired to use non-dimensional time as follows:

$$\tau = \frac{ct}{a}$$

Equation (150), summed through eight modes, is shown in graphical form on Figure 12 for two spatial positions, $\theta = 0$ and $\theta = \frac{\pi}{2}$. Shown also in Figure 12 are the experimental results from [16]. There is good agreement between theory and experiment, particularly at the $\theta = 0$ position. As an added observation, the initial portion of the stress history at the $\theta = 0$ position indicates the effect of "destructive interference" of the modes which can be construed as an index of solution convergence. Note that there is no significant stress until after $\tau = \frac{\pi}{2}$, which, based on elementary wave propagation theory, is the time required for a disturbance to travel 1/4 of the circumference of the ring.

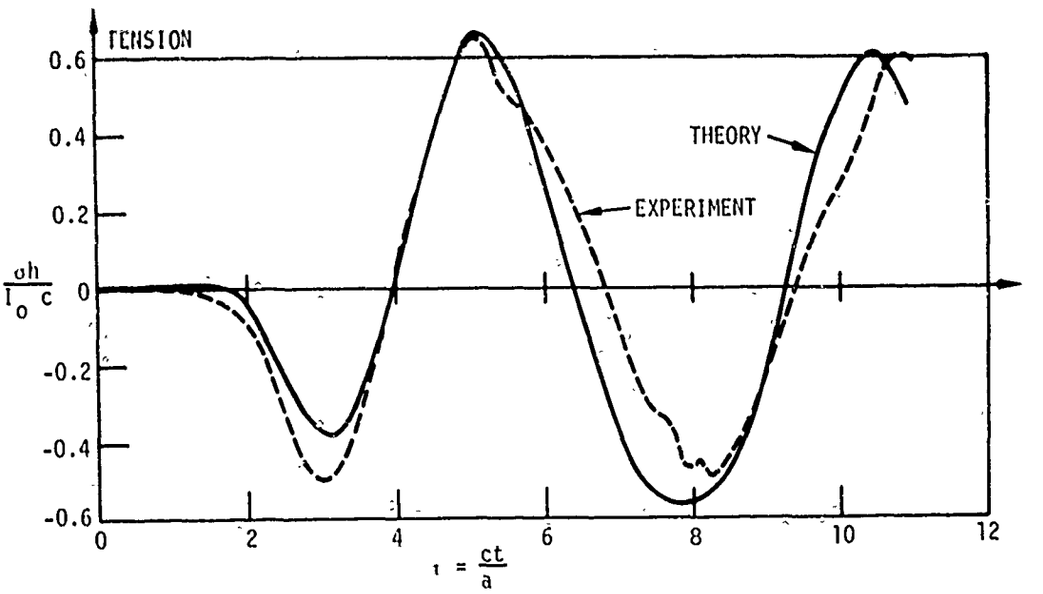

$\theta = 0$, INSIDE RING

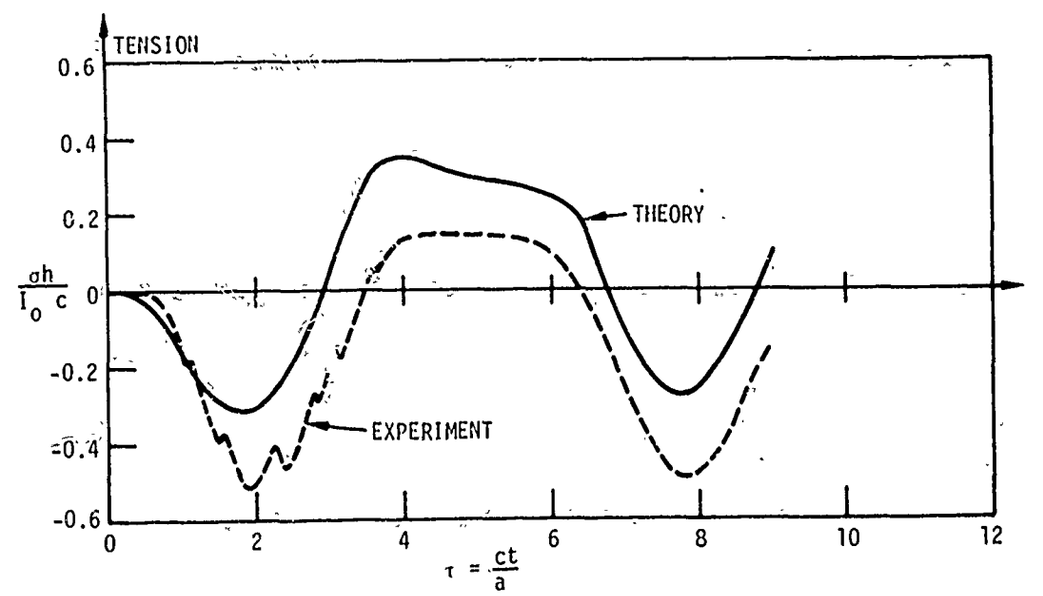

$\theta = \frac{\pi}{2}$, INSIDE RING

Figure 12 - Theoretical and Experimental [16] Stress Histories, R = 0, Z = 0.00011

D. Discussion

In the above analytical solutions the loading given by equations (137) is assumed to occur instantaneously over half the circumference. Such conditions are never physically attainable in experiments since the loading always occurs over a finite period of time. However, if the duration of load application is small in comparison with the period of the lowest natural frequency of the system, then an instantaneous or impulse type load condition is usually considered to be a valid approximation to the physical problem. In Case 3 above, where a flyer plate impacts a ring in air, an assumed instantaneous loading is valid as evidenced by the agreement between theory and experiment shown in Figure 12. For the Navy experiments, Cases 1 and 2, an impulse type loading seemingly is more of an approximation to the actual conditions and further explanation is necessary. A strong, rapidly decaying shock-wave interacting with a structure submerged in a fluid medium is an extremely complex non-linear problem in the complete sens . The principal cause of non-linearity is the occurrence of cavitation or separation between the structure and surrounding fluid after the shock-wave arrives at the structure. Cavitation occurs because of the inability of the fluid to withstand any appreciable negative pressure resulting from the radiated rarefaction wave. It is largely the presence of cavitation, however, that permits the application of an impulse type solution to describe the response of the cylinder for early times. From experiments [21], it has been observed that the first peak velocity, $\dot{w}_0$, occurs very early (on the order of 1/2 msec) after shockwave arrival and can be predicted solely from the shockwave

parameters and shell mass properties without regard to shell stiffness characteristics. During this early time period after shockwave arrival, the first disturbance in the shell has propagated along the circumference in both directions about the initial contact point a distance nearly equal to one-quarter of the circumference of the cylinder. By the time the peak velocity $\dot{\bar{w}}_0$ is reached at the first contact point, a spatial distribution of velocity is present over about one-half the circumference of the shell. For analytical convenience, it is assumed that this initial velocity is spatially distributed in the manner described by equations (137). It is noted that the time required to develop this spatial velocity distribution is small in comparison with the periods of the lowest natural frequencies of either the extensional or flexural classes of vibration. An impulse response solution for this particular problem involves another approximation, which is that the influence of the shockwave in the surrounding water is not accounted for except in the determination of $\dot{\bar{w}}_0$. The effect of the shockwave as it engulfs the cylinder is considerably reduced because the faster moving disturbance in the shell creates a precursor or a radiated wave in the water ahead of the free-water shockwave. Thus the water is disturbed ahead of the propagating shockwave which lessens the shockwave influence on the cylinder. Two other factors which tend to reduce the effect of the shockwave are the natural decay in amplitude of the wave front as the distance from the source is increased, and the changing angle of incidence of the wave front with the cylinder. On the far side of the cylinder, or shadow zone, the wave is considerably diffused due to diffraction over the cylinder as an obstacle, and due to the

effect of the radiated wave as described above. From experimental [21] pressure measurements taken near the fluid-cylinder interface, cavitation has been observed to begin at the time $\dot{\bar{w}}_0$ is reached and persist for a duration of several milliseconds. During this early period of time, the cylinder behaves as though it were decoupled from the surrounding fluid medium. It is this decoupling that permits the early response features of the cylinder to be predicted reasonably well (see Figure 11) by the theory described herein. In other situations where little or no cavitation occurs the present theory would be less applicable, if at all.

V. DISCUSSION

Technical aspects of the natural vibration and impulse response solutions have been discussed as appropriate in previous chapters. The discussion in this chapter will pertain to implications of the theoretical results with respect to state of the art, current applications and future research.

The solution of a fundamental problem has been obtained herein, thus the state of the art in the area of vibrations of mass-loaded structures has been advanced. Heretofore, as noted in the literature survey, the only solutions available, other than a simplified theoretical treatment, were those obtained by approximate methods of analysis. With the solution for the natural vibrations, a variety of initial value and forced vibration problems can now be approached in a more rigorous manner. An application of the theory to an initial value problem was demonstrated in the previous chapter and judging by the recent increased interest shown in the literature, there are several other problem areas in which the present theory would be directly applicable.

The effect of imperfections on the vibrations of bodies of revolution is a problem area of basic physical importance. Preliminary experimental investigations [1,2,3] into the vibrations of imperfect bodies of revolution have shown that the presence of a small asymmetry tended to resolve a single natural frequency into two nearby values. The larger the asymmetry or irregularity, the farther apart and more distinct the frequencies. Resonance tests have revealed the existence

of so-called preferential planes, i.e., if the body was excited in one of these planes, only one resonance peak occurred, but if excited at another position around the body, two peaks were observed for the same mode number. For a body of revolution with a mass imperfection, the results of this investigation tend to support such experimental phenomena since the symmetrical and anti-symmetrical branches of the same mode were found to have different natural frequencies. A systematic combined theoretical and experimental study of such phenomena would be a contribution as apparently no such study has been reported in the literature. The governing equations and their solution given herein could be utilized in a theoretical study of the effects of combined mass and elastic imperfections for the two dimensional problem.

With regard to the problem of an underwater shock wave interacting with a cylinder, some further effort is needed to establish the range of applicability of an impulse type solution as presented herein. If large non-linear cavitation effects are not present, then linear acoustic theory, recently extended by Huang [22], would be more appropriate to this problem. To determine their range of validity, parametric studies should be made with both theories, impulse response and acoustic interaction, for comparison with various experimental results.

Concerning current applications of the theory, perhaps the most important aspect from an engineering standpoint is that the solution can serve as a base for comparison with approximate analytical methods, such as the finite element. Such methods offer a means for obtaining

practical solutions of more complex problems. For example, an analytical study of the vibrations of a cylinder containing several lumped masses and attached mechanical systems would be intractable except by an approximate approach. In this connection, it is noted that in an approximate energy approach to such problems, improved trial functions would be available since the general character of the solution would be known from the present theory.

As the first extension of the theory for future research, it would be desirable to include rotatory inertia of the added mass. In principle, this additional feature would offer little analytical difficulty, and the solution would be more realistic, particularly for anti-symmetrical branch motions. Another future research effort that should be considered is extension of the theory to include rotatory inertia and shear deformation effects in the shell. Extension of the theory in this manner, whether done approximately or by using higher order shell equations, would involve considerable analytical effort; however, the inclusion of such effects would offer a more accurate account of the coupling of the extensional and flexural motions as shown in Figure 7.

To obtain a better physical representation of a large added mass, the theory should be extended to include the added mass distributed over a finite length of the circumference, or a finite length rigid inclusion, rather than concentrated at a point on the circumference. If considering the problem of a mechanical system attached to the cylinder, then a more accurate treatment would be to model both mass and elastic properties of the system, instead of just the mass alone.

For each of the problems mentioned above, the governing equations and their solution, equations (10) and (11), would be applicable, although the eigenvalue problem would change due to differences in boundary conditions.

The theory could perhaps be extended to other more complex problems, such as a finite cylindrical shell with an attached mechanical system, to mention one, but an extensive preliminary effort would have to be made in each case to determine if a rigorous analytical treatment would be tractable.

VI. SUMMARY

The complete plane strain solution was obtained for the natural vibrations of a thin circular cylindrical shell containing an added concentrated line mass. For a particular mode, four distinct solution states were found to exist, a symmetrical and anti-symmetrical branch for each class, flexural and extensional. Significant features revealed by this investigation were the difference in frequency and mode shape of each solution state and the presence of coupling between the flexural and extensional classes, particularly noticeable in the extensional class mode shapes. The solution for the case of a uniform cylinder was obtained from the general solution by taking the added mass to be zero. For the uniform cylinder, the frequencies of each branch of the same class were, as expected, the same. The influence of the added mass was determined by comparing numerical solutions with and without the mass. It was found that with the added mass the natural frequency was reduced for each solution state with greater reduction occurring in the flexural class than in the extensional class for a particular mode. The results of an experimental natural vibration study [8] were found to be in general agreement with the theory.

Using the natural vibration solution, the general impulse response solution for arbitrary initial conditions was obtained by normal mode theory. From the general solution, numerical solutions for specified initial conditions were obtained and compared with the results of several experimental studies [15,16,20]. In all cases, the theory was found to agree reasonably well with experiment. The major influence of the added mass on the impluse response was found to be an

increased participation of the rigid body translation and flexural class modes, and decreased participation of the extensional class oscillatory modes.

In the discussion of the previous chapter, several direct practical applications of the theory were mentioned. The theory would be applicable in basic studies of the vibrations of bodies of revolution containing certain imperfections, in predicting the early response of submerged cylinders to shock waves in the presence of cavitation, and as a base for comparison with approximate analytical methods. Discussed also were areas of future research for extension of the theory so that it would be physically more meaningful in certain future applications. In this regard, it was pointed out that an effort should be made to include rotatory inertia of the added mass and to consider rotatory inertia and shear deformation effects in the shell. It was also pointed out that for some situations, more realistic models of the attached mass other than as a concentrated line mass should be considered as topics for future research.

ACKNOWLEDGMENTS

The author acknowledges the staff of the Naval Ship Research and Development Center, in particular Dr. H. M. Schauer and Mr. R. D. Short, for initial guidance in this research effort, and Dr. R. Chicurel and other faculty members of the Engineering Mechanics Department, Virginia Polytechnic Institute, for their suggestions and guidance in the preparation of this thesis.

REFERENCES

1. Tobias, S. A., "A Theory of Imperfection for the Vibrations of Elastic Bodies of Revolution," Engineering, Vol. 172, No. 4470, pp 409–411 (1951).

2. Fung, Y. C. et al., "On the Vibrations of Thin Cylindrical Shells under Internal Pressure," Journal of the Aeronautical Sciences, Vol. 24, No. 9, pp 650–670 (1957).

3. Cohen, D. S., "Vibration and Sound Radiation Measurements of Stiffened Cylindrical Shells," David Taylor Model Basin Report C-1305 (Apr 1962) CONFIDENTIAL.

4. Den Hartog, J. P., "Vibrations of Frames of Electrical Machines," Transactions of the ASME, Vol. 50 (1928).

5. Palmer, E. W., "The Influence of a Mass on the Free Flexural Vibrations of a Circular Ring," Master's Thesis, Virginia Polytechnic Institute, Blacksburg, Va. (Dec 1962).

6. Michalopoulos, C. D. and Muster, D., "The Effect of Plane-Symmetric Mass Loading on the Response of Ring-Stiffened Cylindrical Shells," Univ. of Houston, Dept. of Mechanical Engineering, Tech. Report 4 (Aug 1966).

7. Ojalvo, I. U. and Newman, M., "Natural Vibrations of a Stiffened Pressurized Cylinder with an Attached Mass," AIAA Journal, Vol. 5, No. 6, pp 1139–1146 (Jun 1967).

8. Lee, S. Y. et al., "Mass-Loading Effects on Vibrations of Ring and Shell Structures," Space Division, North American Rockwell Corp., SD 68-29 (Feb 1968).

9. Thornton, E. A., "Applications of a Generalized Integral Transform to Vibrations of Continuous Media," Ph.D. Dissertation, Virginia Polytechnic Institute, Blacksburg, Va. (May 1968).

10. Palmer, E. W., "The Shock Environment of Submarine Pressure-Hull Penetrations under Explosion Attack," Shock and Vibration Bulletin No. 33, Part I, pp 57–63 (Feb 1964).

11. Humphreys, J. S. and Winter, R., "Dynamic Response of a Cylinder to a Side Pressure Pulse," AIAA Journal, Vol. 3, No. 1, pp 27–32 (Jan 1965).

12. Sheng, J., "The Response of a Thin Cylindrical Shell to Transient Surface Loading," AIAA Journal, Vol. 3, No. 4, pp 701–709 (Apr 1965).

13. Johnson, D. E. and Greif, R., "Dynamic Response of a Cylindrical Shell: Two Numerical Methods," AIAA Journal, Vol. 4, No. 3, pp 486–494 (Mar 1966).

14. Flugge, W., "Stresses in Shells," Springer-Verlag, Berlin, p. 219 (1960).

15. Bloodgood, V. G., "Theoretical Investigation of the Initial Response of a Thin Ring to a Radial Shock Pulse," Master's Thesis, Virginia Polytechnic Institute, Blacksburg, Va. (Jun 1967).

16. Private correspondence from W. E. Alzheimer, Div. 1541, Sandia Corporation, Albuquerque, New Mexico (Aug 1969).

17. Baron, M. L. and Bleich, H. H., "Further Studies of the Response of a Cylindrical Shell to a Transverse Shock Wave," Columbia Univ. Tech. Report 10 (Dec 1953).

18. Love, A. E. H., "A Treatise on the Mathematical Theory of Elasticity," Fourth Edition, Dover Publications, New York (1944).

19. Timoshenko, S., "Vibration Problems in Engineering," Third Edition, D. Van Nostrand Company, New York (1955).

20. Test 5961, Velocity Meter 2, Underwater Explosions Research Division (Code 773), Naval Ship Research and Development Center, Portsmouth, Virginia 23709.

21. Palmer, E. W., "A Method for the Shock Design of Submarine Pressure Hull Attachments (U)," NSRDC Report C-2537 (Jan 1968) CONFIDENTIAL.

22. Huang, H., "Exact Linear Analysis of the Transient Response of an Elastic Cylindrical Shell of Infinite Length to Plane Underwater Shock Waves," NAVSHIPRANDLAB Annapolis Report MACHLAB 163 (Jul 1969).

UNCLASSIFIED

Security Classification

DOCUMENT CONTROL DATA - R & D

(Security classification of title, body of abstract and indexing annotation must be entered when the overall report is classified)

1 ORIGINATING ACTIVITY (Corporate author) Naval Ship Research and Development Center Washington, D. C 20034	2a. REPORT SECURITY CLASSIFICATION UNCLASSIFIED 2b. GROUP

3 REPORT TITLE

THE INFLUENCE OF ADDED MASS ON THE NATURAL VIBRATIONS AND IMPULSE RESPONSE OF LONG, THIN CYLINDRICAL SHELLS

4 DESCRIPTIVE NOTES (Type of report and inclusive dates)

5 AUTHOR(S) (First name, middle initial, last name)

E. W. Palmer

6 REPORT DATE October 1970	7a. TOTAL NO. OF PAGES 74	7b. NO. OF REFS 22
8a. CONTRACT OR GRANT NO b. PROJECT NO SF 35.422.110 Task 15041 c. d	9a. ORIGINATOR'S REPORT NUMBER(S) 3395 9b. OTHER REPORT NO(S) (Any other numbers that may be assigned this report)	

10 DISTRIBUTION STATEMENT

This document has been approved for public release and sale; its distribution is unlimited.

11 SUPPLEMENTARY NOTES	12. SPONSORING MILITARY ACTIVITY Naval Ship Systems Command

13. ABSTRACT

The plane strain solution is obtained for the natural vibrations and impulse response of a thin circular cylinder containing an added line mass. The solution for a uniform cylinder is derived by taking the added mass to be zero. Numerical calculations of the frequencies and mode shapes for several of the lower modes are presented in graphical form for various values of the added mass. The general impulse response solution for arbitrary initial conditions is obtained by normal mode theory. For both the natural vibrations and impulse response, the theory is found to be in reasonable agreement with available experimental results.

In a particular mode, four distinct solution states are found to exist: a symmetrical and anti-symmetrical branch for each class of vibration, flexural and extensional. Noteworthy features revealed by this investigation are the difference in frequency and mode shape of each solution state and the presence of coupling between the flexural and extensional classes, particularly noticeable in the extensional class mode shapes. In comparing impulse response solutions for velocity with and without the added mass, the major influence of the added mass is found to be an increased participation of the flexural class modes, including the rigid body translation, and decreased participation of the extensional class oscillatory modes.

DD FORM 1 NOV 65 1473 (PAGE 1)

S/N 0101-807-6801

UNCLASSIFIED

Security Classification

14 KEY WORDS	LINK A		LINK B		LINK C	
	ROLE	WT	ROLE	WT	ROLE	WT
Natural vibrations						
Impulse response						
Cylinder with attached mass						
Thin shells						
Comparison with experiment						